DESY-2004-06
CPPM-H-2003-01
January 2004

Isolated Lepton Production at Colliders

Cristinel Diaconu[1]
Centre de Physique des Particules de Marseille
Case 902 , 163 Avenue de Luminy 13288 Marseille cedex 09, France
diaconu@cppm.in2p3.fr

The production of isolated leptons with high transverse momentum in high energy ee, pp or ep collisions is reviewed. The leptons are produced either through boson splitting or by boson-boson collision and yield experimentally simple and spectacular topologies which can be exploited to validate the Standard Model or to search for new phenomena.

[1]Habilitation à diriger des recherches, December 15, 2003

Contents

1 Leptons from Collisions

1.1 Definition

The major goal of the high energy particle colliders is to investigate the structure of the matter at very short distances. The signature of the processes that access the shortest distances is the large transverse momenta of the produced particles in the final state. In addition, the creation of new particles, of different type form the colliding particles, provides an useful tool for investigating the nature of the high energy phenomena.

During the collision process, the beam particles can act as composed systems. The main interaction, also called “hard scattering”, takes place actually between two constituents or “partons”. This is obvious for the case of the proton, for which most phenomena occuring in collisions can be explained by the proton’s quarks or gluons. Partially this is also the case for the electron or even for the photon, as will be explained below.

In particle collisions, the primary (or “hard”) processes can be classified in several cases.

- **A** “elastic” scattering of two elementary partons $ab \to ab$ (for instance the Bhabha scattering $e^+e^- \to e^+e^-$ or the deep inelastic scattering $eq \to eq$).
- **B** “quasi-elastic hard scattering” where the two initial partons are also in the final state, but new particles are created $ab \to abcd$. This is the case for instance in the four fermion production at LEP if the electron-positron pair is found in the final state: $e^+e^- \to e^+e^- f\bar{f}$.
- **C** “inelastic hard scattering” where the initial state partons are transformed into new particles like for instance $ab \to a'b'$ (for instance the Drell–Yan process $q\bar{q} \to \ell^+\ell^-$), with possibly multiplication of final state particles by the mechanism related to the previous point: $ab \to a'b'cd$ (for instance $e^+e^- \to \mu^+\mu^- q\bar{q}$).

In this paper we are going to review processes that yield new particles different from the colliding partons (processes of type **B** and **C**). In addition we focus on the production of leptons in the final state. These processes are defined by the condition:

$$\Delta N_L = N_L^f - N_L^i > 0,$$

where N_L^i (N_L^f) is the number of charged or neutral leptons in the initial (final) state.

The production of isolated leptons at high transverse momentum in high energetic collisions is particularly interesting due to the clean experimental signature. The production mechanisms in the Standard Model framework include weak boson decays or boson-boson fusion, as will be described below.

The high P_T lepton production reveals important information related to the matter structure at short distances:

- gauge structure and coupling strengths of the Standard Model;
- composed particles structure: proton structure and study of hadronic fluctuation of the photon;
- search for physics beyond the Standard Model.

In this paper we summarize the lepton production in high energy collisions at present colliders. In the following, we will shortly present the production mechanisms and the experimental setups at LEP, HERA and Tevatron.

1.2 Basic lepton production mechanisms in the Standard Model

In the Standard Model leptons couple to the photon and to the weak boson W and Z which in turn couple to initial state partons that can be of different nature than the produced leptons. It is important to note that leptons can only be produced in pairs in the Standard Model framework. The leptonic number is conserved and ΔN_ℓ can only be an even integer.

There are two production mechanisms that may produce a pair of leptons.

boson conversion

A pair of leptons can be issued from a real or virtual boson γ^*, $W^{(*)}$, $Z^{(*)}$ or by the decays of an on-shell weak boson W or Z. The lepton pair production at sufficient high energies is the natural signature for weak boson production and used in the experimental analyses of the weak bosons properties. The lepton–boson couplings to charged or neutral bosons are described below [1].
The charged current coupling is given by:

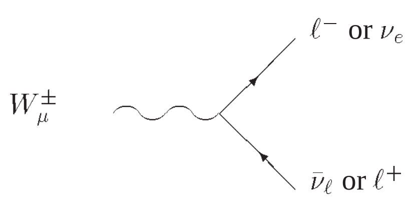

$$ie\gamma_\mu(1-\gamma_5)\frac{1}{2\sqrt{2}\sin\theta_W}$$

ℓ is e, μ or τ. Due to the $1-\gamma_5$ factor, only left-handed leptons are created or annihilated at this vertex. There is no charged current interaction between leptons of different flavours, which correspond to no mixing in the leptonic sector, in contrast to the quark sector where the Cabibbo-Kobayashi-Maskawa matrix element is an extra factor in the coupling. This assumption was based on the fact that neutrinos were believed to have no mass. The recent experimental evidence for non-zero neutrinos masses opens the possibility of some mixing also in the leptonic sector.

The photon couples to the electrical charge of the lepton:

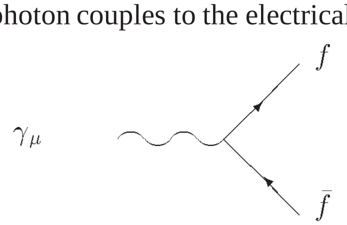

$$-ieQ_f\gamma_\mu$$

The weak interaction by neutral current is described by:

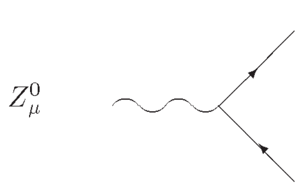

$$ie\gamma_\mu(v_f - a_f\gamma_5)$$

where the coupling constants are :

$$v_f = \frac{I_3 - 2Q_f \sin^2\theta_W}{2\sin\theta_W\cos\theta_W}, \qquad a_f = \frac{I_3}{2\sin\theta_W\cos\theta_W}$$

with θ_W the weak mixing angle, Q_f fermion charge and I_3 the third component of the weak isospin ($-1/2$ for charged leptons and $+1/2$ for the neutrinos). In the Standard Model the neutral currents do not mix flavours, an assumption based on present experimental non-observation of processes with flavour changing neutral currents (FCNC). The neutral current weak interactions trough a Z involve a superposition of left– and right–handed charged leptons. This leads to interesting helicity effects in the experimental observables like charge/spin asymmetries.

boson-boson fusion

In this case two bosons merge to produce a pair of leptons as showed below. The most common mechanism in this case is the photon–photon collision. The photon fusion with a weak boson is not favoured within the Standard Model due to the large weak boson mass.

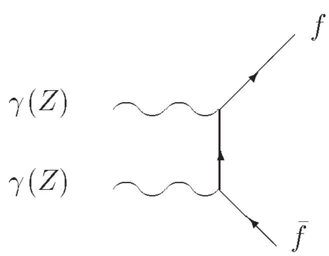

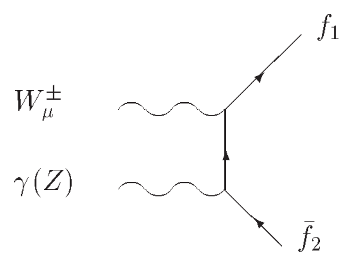

1.3 The colliders and the ingredients

The present study covers the three highest energy colliders LEP (e^+e^-) HERA ($e^\pm p$) et Tevatron ($p\bar{p}$), the characteristics of which are summarized in table 1.1. In total, LEP experiments accumulated approximately 3.5 fb^{-1} for centre-of-mass energy ranging from 89 to 209 GeV. In their first running period, HERA and Tevatron experiments only collected 0.25 fb^{-1}, respectively. The second phase, recently started both at DESY and Fermilab, should bring the available luminosities in ep and $p\bar{p}$ collision modes close to the LEP value, for centre-of-mass energies of 319 GeV (HERA) and 1.96 GeV (Tevatron).

The highly energetic collisions of particle beams lead to a variety of primary hard scattering processes. Besides the direct interaction between the colliding particles, the initial state processes (radiation, parton substructure etc.) can lead to a picture where the intial beams produce secondary beams of different particles that enter the true hard scattering. For instance, the direct electron-proton interaction at HERA may take place in elastic scattering. In Deep Inelastic Scattering (DIS), the proton is seen as a bag filled with quarks or gluons and HERA collides (in a “second” mode) electrons with quarks or electrons with gluons. In the same way at LEP the flux of real photons from initial state radiation on one side can

	HERA	**LEP**	**TEVATRON**
Beams	$e^{\pm} - p$	$e^{+} - e^{-}$	$p - \bar{p}$
Expt.	H1 ZEUS	ADLO	CDF,D0
$\mathcal{L}$/expt.	120 pb^{-1}	800 pb^{-1}	150 pb^{-1}
Future (goal)	HERA II (1 fb^{-1})		run 2 ($4 \div 8$ fb^{-1})

Table 1.1: Summary of LEP, HERA et Tevatron characteristics and performances

Collider	Beams	"Second" mode collisions	Comment
LEP	$e^{+} - e^{-}$		full use of the $\sqrt{s}$
			dominates at high P_T
		$e^{\pm} - \gamma$	
		$\gamma - \gamma$	
HERA	$e^{\pm} - p$		elastic/diffraction
		$e^{\pm} - q$	DIS
		$e^{\pm} - \gamma$	Compton
		$\gamma - q$	
		$\gamma - g$	
		$q - q$	photo–production (from $e \rightarrow \gamma \rightarrow$hadrons)
		$\gamma - \gamma$	
TEVATRON	$p - \bar{p}$		elastic/diffraction
		$q - q$	main collision mode
		$q - g$	for high P_T physics
		$g - g$	for high P_T physics

Table 1.2: Possible parton-parton interactions at colliders with electron and/or proton beams

collide with the electron beam from the other side or with its associated photon beam and therefore LEP can function as $e - \gamma$ or $\gamma - \gamma$ collider.

This "second" mode functionning for the considered colliders is summarized in table 1.3.

Altough this picture of the hard scattering is schematical and incomplete, it helps understanding the main features in the capabilities of the three colliders to test the Standard Model and to search for the new physics. The partonic luminosities [2] are shown in figure 1.1. From that picture one can see for instance that HERA collides electrons with quarks at highest energy and luminosity up to 300 GeV. LEP has the priority on $e - \gamma$ collisions up to its centre-of-mass energy but HERA takes over at higher energies.

The physics potential of a collider with respect to a given process depends on the following three factors:

Luminosity This includes the partonic luminosity as discussed above but also the total integrated collision luminosity, which has to do rather with the existing tehnology for accelerating and colliding a given type of particles.

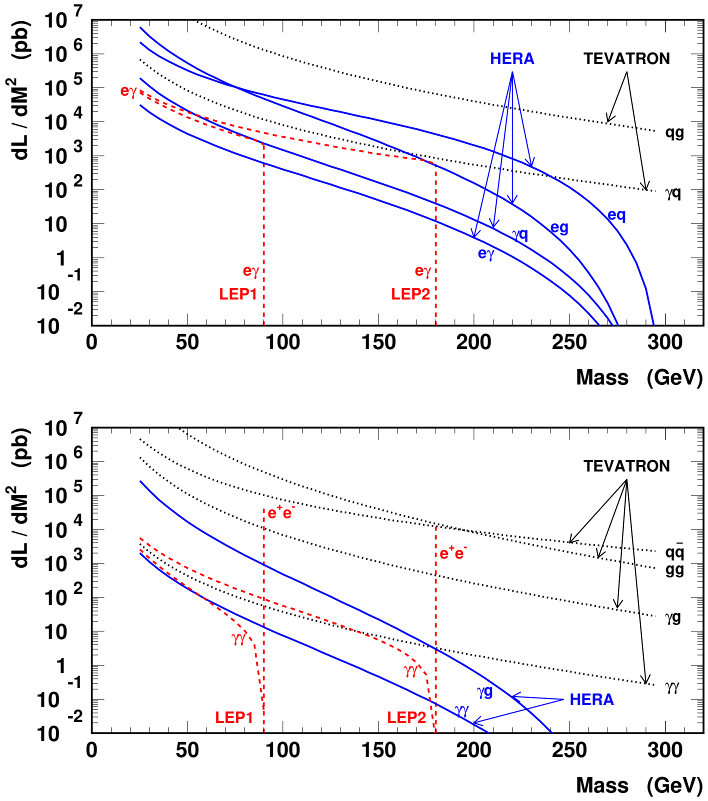

Figure 1.1: Diferential partonic luminosities (dL/dM^2) at LEP HERA and Tevatron as a function of the centre-of-mass energy of the parton-parton collision. In this figure $\sqrt{s}(e^+e^-)_{LEP} = 180$ GeV and $\sqrt{s}(p\bar{p})_{Tevatron} = 1.8$ TeV.

Cross section of the hard scattering. The hard scattering cross section is convoluted with the partonic fluxes and with the experimental acceptance in order to obtain the observed cross section. The higher the cross section, the better the sensitivity of a given collider to the searched process.

Background The observability of the searched process depends on the rate of irreducible Standard Model background processes.

The study of the processes that yield leptons ($\Delta N_L > 0$) is of course dependent on the experimental luminosity. In addition, due to the partonic nature of the interaction at HERA and Tevatron, the effective centre-of-mass energy is reduced and a part of the input energy is lost with the proton remnants. The phase space for particle (lepton) production at high P_T is in this way reduced, in contrast to the LEP case, where most of the time the full available energy is “consumed” for particle production. The factor of ten in collision energy at Tevatron with respect to LEP helps to recover from that handicap, while HERA has only a modest advantage in centre-of-mass energy versus LEP. Conversely, the small production rate within the Standard Model for a given multi-lepton topology product may be useful in the frame of some searches for new physics, where the smaller background increases the sensitivity.

The experimental backgrounds for lepton identification are small at LEP, while at HERA and Tevatron the hadronic processes or the radiative processes with photons in the final state have a larger cross section and represent often a challenge for the lepton identification.

In the next chapter we summarize the main experimental analyses related to the lepton production at LEP, HERA and Tevatron. The possible models and experimental searches of the new physics using high energy lepton signatures are described in the last chapter.

2 Lepton Production in the Standard Model

2.1 Motivation

The measurement of energetic and isolated leptons in the final state provides a useful probe of the underlying processes occuring in high energy collisions. This is due to the following facts:

- The leptons are not sensitive to the strong interactions. The final state interactions are therefore small and well understood within the Standard Model.
- The leptons couple to gauge bosons. Final states containing high energy isolated leptons may signal large boson masses or virtualities. The highly virtual photons resolve the matter to short distances with interesting insight into partonic structure. The leptonic decays of heavy electroweak boson are gold plated channels for further electroweak sector tests.
- In view of searches for non standard phenomena, events with leptons provide a clean signature. The production cross sections are significantly lower than the quark(jet) production in the same mass or P_T range.
- The charge is experimentally accessible for the charged leptons, in contrast with quarks. A high energy neutrinos in the final state signals an underlying charged current interaction or a real $W^{\pm}$ boson produced in the final state. This implies that a final state with high energetic leptons provides a better signature for specific subprocesses of the Standard Model or for signals beyond the Standard Model .

The Standard Model predicts the relationship between the leptonic channels and the hadronic final states. Therefore, if the background from QCD-like processes is not too high, the analysis of leptonic final states is correlated to and complemented by the hadronic channels.

In this chapter the production of high P_T isolated leptons is summarized for the experimental measurements done at LEP, Tevatron and HERA colliders. The production mechanisms within the Standard Model are briefly explained. Possible BSM interpretations of the final states with extra-leptons with high P_T will be discussed in the next chapter.

2.2 High P_T lepton production at LEP

In electron–positron collisions the annihilation process dominates the production rate of high P_T leptons. The e^+e^- pair fuses into a massive boson (γ^* or $Z^{(*)}$) that subsequently materialises into a lepton pair (ΔN_L=0) or a quark–antiquark pair ($\Delta N_L = -2$). The fermion pair production at LEP is an important tool for measuring the electroweak parameters [3]. The measurement of the Z boson mass and width, the hadronic pole cross section o-f Z exchange, the ratios of hadron to lepton cross-sections for the

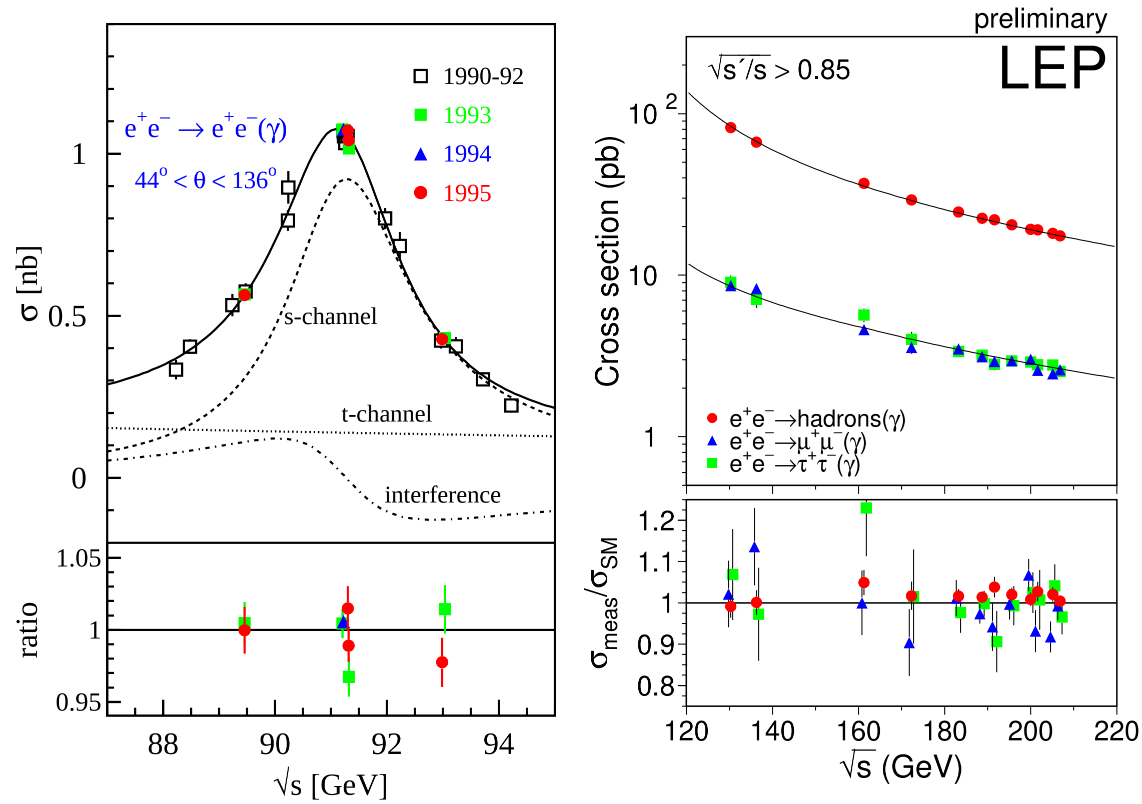

Figure 2.1: Cross section for $e^+e^- \to f\bar{f}$ as a function of center of mass energy measured by LEP experiments around the Z pole (left) and at higher LEP2 energies (right).

three types of leptons and for the b and the c quarks together with the corresponding forward-backward asymmetries are used to extract the Standard Model parameters with high precision [4]. The cross section of fermion pair production as a function of the center of mass energy is shown in figure 2.1 for the centre-of-mass energy around the Z mass (left) and in the higher centre-of-mass energy regime of LEP2 (right).

Within the Standard Model, extra lepton production ($\Delta N_L = 2$) is part of a higher order process ($\mathcal{O}(\alpha^4)$) leading to four fermions in the final state. As an example, the production mechanisms for four charged fermions are shown in figure 2.2 (left). The final state with electrons is described by more diagrams, including the t-channel scattering that is possible only in the $e^+e^- \to e^+e^- ff$ processes. At LEP2 energies, the four lepton production can also proceed through single or double resonant processes with one or two weak bosons (W or Z) in the final state. The cross section of weak boson production at LEP2 energies is illustrated in figure 2.2 (right).

In an electron–positron collider, the partons that enter the hard scattering leading to more than two leptons in the final state can be:

- e^+e^- : up to 4 leptons at high P_T in the final state. The extra pair of leptons is produced during the hard e^+e^- scattering to four particles. The full $2 \to 4$ matrix elements calculation is used for the theoretical calculation of this process. Resonant vector boson production is possible if enough centre-of-mass energy is available. The final state is either fully detected or, in the case

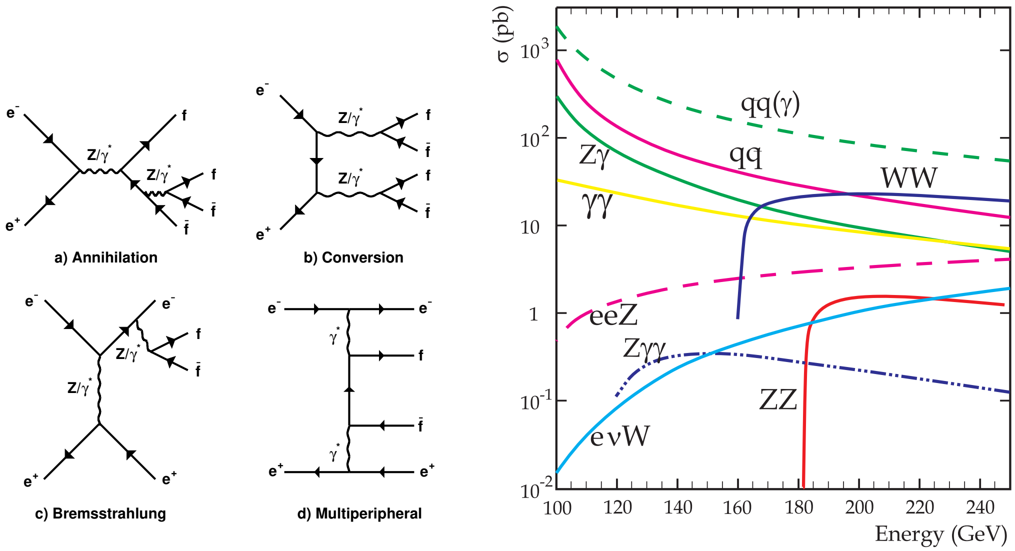

Figure 2.2: Four fermions production mechanisms in e^+e^- collisions for the neutral current production (left) and Standard Model fermion pair and boson pair production cross section as a function of $\sqrt{s}$ at LEP2 energies (right).

of neutrinos in the final state, the energy–momentum conservation may be used to constrain the kinematics.

- $e\gamma$: one of the incident electrons escapes down the beampipe after producing the interacting photon. Besides the classical QED Compton scattering $e\gamma \to e\gamma$, multilepton final states can be produced through the so-called electroweak Compton mechanism $e\gamma \to e\gamma^*$ or $e\gamma \to eZ$, with subsequent boson conversion into a lepton pair. In this case three leptons of the final state are usually in the detector acceptance. The calculation relies on a convolution of photon flux with the electroweak Compton scattering matrix elements. The process is tagged either by the presence of an electron close to the beam pipe or by the missing energy aligned with the beam direction, due to the escaping electron. The charged current EW Compton process $e\gamma \to \nu W$ is also possible. The electroweak Compton scattering provides the main mechanism of single vector boson production at LEP.

- $\gamma\gamma$: two leptons in the final state. At high transverse momentum, this contribution is modest with respect to the s–channel di-lepton production. However, it can well be measured by using "tagged" events, where at least one of the scattered electrons is measured in a low angle detector near the beam pipe.

The neutral current interactions lead to final states with charged leptons only in the final states in all cases except for the Z boson conversion into a neutrino pair. The charged current interactions, mediated in the Standard Model by W bosons, lead to final states containing neutrinos.

From the experimental point of view, the excellent hermeticity and tracking performance allow to detect charged leptons with transverse momenta as low as 1 GeV and to signal the presence of an undetected particle by the missing transverse energy down to a few GeV. Depending on the analysed final state, the energy–momentum conservation is used to improve the resolution or to separate the signal from the background.

In the following, main topologies with charged or neutral leptons in the final state are described. After a short insight into a LEP1 study of events with four fermions, we will concentrate on LEP2 data obtained at highest e^+e^- collision energies.

2.2.1 Four fermion production at LEP1

Four fermion production at LEP I is based on final state topologies with two leptons plus two other fermions $\ell^+\ell^- f\bar{f}$. The ALEPH collaboration studied events in which, besides two charged leptons used as a tag, two other fermions are identified [5]. Using tracking information, low multiplicity events, also called $\ell^+\ell^- V$, are selected. Part of this sample is identified as four-lepton events. The rest is attributed to the production of two hadrons $\pi^+\pi^-$ or K^+K^- in addition to the lepton pair. The hadron pair may originate from the decay of the resonance formed by the quark-antiquark pair produced in the final state.

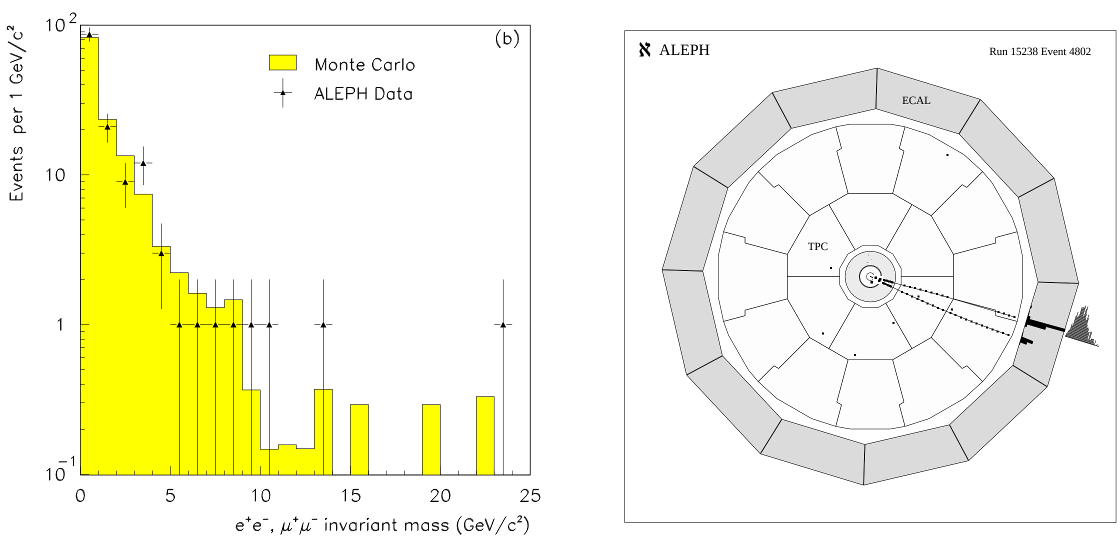

Figure 2.3: Minimal di-fermion invariant mass distribution for events with four fermions at LEP (left) and a candidate for $e^+e^- \to \nu\bar{\nu}e^+e^-$ process (right).

This study revealed a good agreement between the data and the Standard Model prediction. The minimum di-fermion invariant mass is shown in figure 2.3 (left). The selected events are concentrated at low values consistent with a production mechanism based mainly on γ^* internal conversion. Besides events with four charged fermions, evidence for the production of charged leptons in events with neutrinos has also been found – an event with two charged leptons associated with large missing energy is shown in figure 2.3 (right).

2.2.2 Events with charged leptons at LEP2

The search for the process $e^+e^- \to 4\ell^\pm$ relies on the well understood lepton identification. As an example, we consider the flavour independent analysis performed by the DELPHI collaboration [6]. The analysis is part of a study of four fermion production through neutral current interactions at $\sqrt{s} =$

$183 \div 208$ GeV. The distributions of the minimal and maximal invariant mass of the lepton pairs in the event are shown in figure 2.4(left). The Z peak is observed in the maximal mass distribution.

The four charged leptons final state is a rather rare process at LEP. For instance, in the flavour-blind analysis (including therefore electrons, muons or taus among the four leptons in the final state) only 16 events were selected in the data compared with a prediction of 14.6 from the Standard Model in the data sample corresponding to an integrated luminosity of 221 pb^{-1} with $\sqrt{s} = 204 \div 209$ GeV.

The total cross section of four lepton production was measured at highest LEP2 centre-of-mass energies in the range from 183 to 208 GeV. The result in the highest energy bin is $\sigma_{204-208} = 0.55^{+0.15}_{-0.13} \pm 0.04$ pb for the flavour blind measurement of leptons with $|\cos\theta| < 0.98$.

The contributions of different poles can be studied if the interference effects are neglected. However, the pure leptonic channel is not well suited for separating ZZ, $Z\gamma^*$ and $\gamma^*\gamma^*$ contributions due to the low statistics. The production of a pair of quarks together with a pair of leptons is included in the analysis by using $e^+e^-q\bar{q}$, $\mu^+\mu^-q\bar{q}$ and $\nu\bar{\nu}q\bar{q}$ final states. The purely hadronic final state $q\bar{q}q\bar{q}$ (four jets) is hampered by the background from QCD processes or WW pair production and cannot be used for NC four fermion production studies.

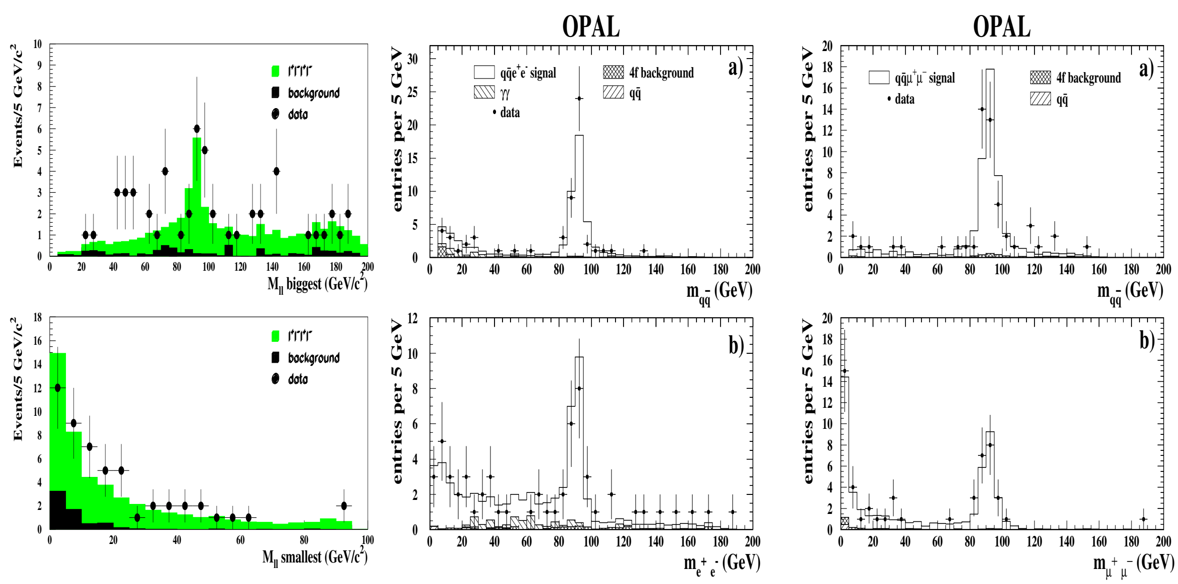

Figure 2.4: Maximum and minimum di-lepton invariant mass distribution for four lepton events detected with a flavour independent method by DELPHI(left). Invariant mass of same flavour fermion pairs in $e^+e^-q\bar{q}$ (center) and $\mu^+\mu^-q\bar{q}$ (right) channels(from OPAL analysis).

Figure 2.4 shows the di-fermion invariant mass distributions obtained in a similar study done by the OPAL collaboration [7]. A significat peak at Z mass due to resonant production $Z \to f\bar{f}$ is visible for both channels and both fermion pairs. The low mass peak due to internal conversion $\gamma^* \to f\bar{f}$ is only visible in $M_{\mu\mu}$ and M_{ee}, while it is supressed by the analysis cuts for the other distributions. No other significant peak, possibly due to a new boson, is found.

The cross sections corresponding to the semileptonic channels $eeqq$ and $\mu\mu qq$ for various production mechanisms are extracted by using a fit of the invariant mass spectra. The contribution from non-resonant process $\sigma_{\gamma^*\gamma^*}$, from semi-resonant process $\sigma_{Z\gamma^*}$ and from double resonantσ_{ZZ} are measured. The t-channel contribution is measured in the $eeqq$ channel. The results are [6]:

$$
\begin{aligned}
&\sigma_{Z\gamma^*} = 0.129 \pm 0.020 \text{ pb},\\
&\sigma_{ZZ} = 0.029 \pm 0.006 \text{ pb},\\
&\sigma_{\gamma^*\gamma^*} = 0.017 \pm 0.008 \text{ pb and}\\
&\sigma_{t-channel} = 0.245 \pm 0.045 \text{ pb (for electrons).}
\end{aligned}
$$

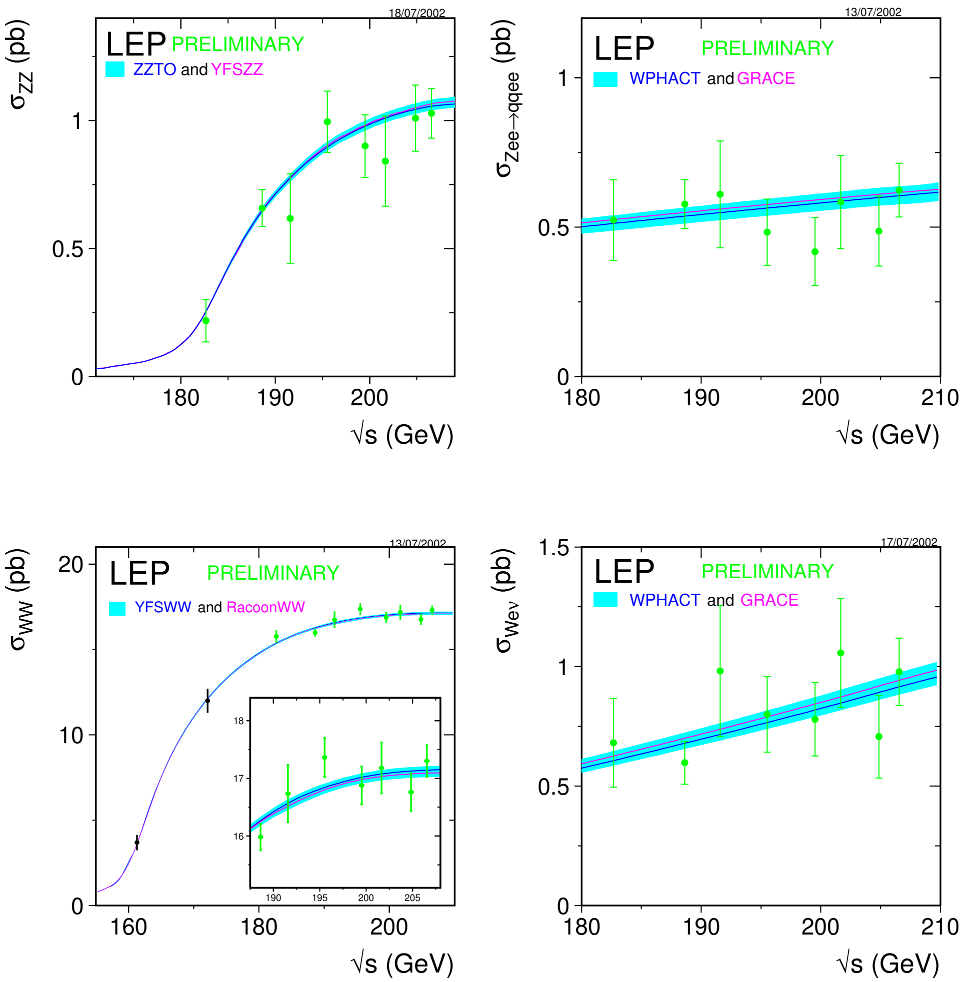

Figure 2.5: The cross sections of weak boson(s) production at LEP as a function of $\sqrt{s}$.

The production of Z bosons pairs is possible at LEP in the highest centre-of-mass energy range. The cross section of Z boson pair production has been measured by LEP collaborations and is presented in figure 2.5(up left). The raise around the kinematical threshold $\sqrt{s} \simeq 2M_Z$ is observed. At highest energy the Z pair production cross section is around 1 pb.

Three leptons at high P_T in the final state

Events with three visible leptons are produced if one of the beam electrons is scattered at low angles and escapes down the beam pipe. In this configuration, the virtuality of the photon emitted by this low angle electron is close to zero and therefore the photon is quasi-real. The corresponding interaction mechanism is the EW Compton scattering $e\gamma \to e\gamma^*/Z$. This mechanism is responsible for single Z boson production at LEP. The final state consists of a low energy electron recoiling against a pair of leptons or jets. The missing momentum in the event should point along the beam direction, corresponding to the lost electron.

The contribution from γ^* and Z can be separated by using the invariant mass spectrum of the boson candidate decay $\gamma^*/Z \to f\bar{f}$ [8, 9]. Low invariant masses of the boson candidate, typically below 60 GeV, are dominated by the non-resonant contribution from γ^*, larger masses are due mainly to the single Z production. The combined measurements of the single Z production as a function of the LEP center of mass energy is presented in figure 2.5(up right). The cross section is defined for the hadronic decay channel of the Z boson and slowly increase as a function of centre-of-mass energy. At highest LEP energy $\sigma_{Zee\to qqee} = 0.6$ pb.

Charged lepton pairs produced in $\gamma\gamma$ collisions

At e^+e^- colliders, leptons pairs can also be produced in $\gamma\gamma$ collisions. This process allows for both Standard Model tests and searches for new phenomena coupled to the two photon collisions [10, 11]. The fermion pair production mechanism can be understood from the diagram d) in figure 2.2. The incident electrons are scattered at low angles and are most of the time lost down the beampipe. However, in order to separate this process from the s–channel annihilation, the “tagged” events are analyzed for which one of the scattered electrons is detected in the sub-detectors situated close to the beam pipe or at low angle in the main calorimeter.

The production of muon pairs in $\gamma\gamma$ collisions allows to study QED up to the fourth order of α. This process has been studied by DELPHI [12] using LEP1 data. The selected sample contains single tag events only, in order to insure that one of the incoming photons is real, i.e. its virtuality $Q^2 \simeq 0$. The virtuality of the other photon is calculated from the tag electron and is in the range $Q^2 = 2.5 \div 750$ GeV^2. The muons with transverse momenta up to 20 GeV are observed in this sample. This analysis allows the measurement of the leptonic photon structure function $F^{\gamma}_{2,\ell}$. The angle between the di-muon plane and the plane formed by the four vector of the tag electron and the beam direction is sensitive to the helicity structure of the photon–photon interaction. The ratios of the helicity related structure functions F_2^A and F_2^B to $F^{\gamma}_{2,\ell}$ are measured from this azimuthal correlations and found in good agreement with the QED prediction.

Using the same technique to tag the photon–photon collision by the low angle electrons, the $\gamma\gamma \to q\bar{q}$ process can be studied by events with hadrons in the final state. The hadron production in $\gamma\gamma$ collisions is a laboratory for QCD studies and the kinematical variables from the data are compared with the prediction from models or NLO-QCD calculation [13,14,15]. The modelling of the hadronic final state is of interest also for the production by this mechanism of high mass states decaying to hadrons. However, the effective centre-of-mass energy is lower than from the direct e^+e^- collisions and no anomaly has been reported for this type of events. The photon structure is studied in deep inelastic $e\gamma$ scattering [16].

2.2.3 Events with charged leptons and missing energy at LEP2

The production of events with high energy leptons and missing energy at LEP proceeds mainly through W bosons. The contribution of events in which the missing transverse momentum originate from $Z \to \nu\bar{\nu}$ is usually small and it will not be discussed here [1].

Events with one prominent lepton and missing transverse energy

In the Standard Model framework, events with one charged lepton and missing transverse energy are produced in e^+e^- collisions through the production of single W bosons. In this case, one of the incident electrons is scattered at low angles and escapes down the beampipe ($|\cos\theta_e| > 0.95$). The basic interaction is a charged current electroweak Compton scattering $e\gamma \to \nu W$ with a subsequent leptonic decay of the W boson. In addition to this mechanism, the production of single W bosons involves the triple gauge coupling γWW ($\gamma + W \to W$). The peripheral contribution from $\gamma - W$ fusion into a $\ell^\pm\nu$ pair via a t-channel neutrino exchange corresponds to the non-resonant continuum.

The single W production in $e\gamma$ collisions has been measured including the hadronic channel $W \to q\bar{q}$. The W identification is rather loose (cut on lepton energy $E > 20$ GeV in the leptonic channels or a cut on di-jet mass > 45 GeV in the hadronic channel). The measured cross section as a function of $\sqrt{s}$ and is shown in figure 2.5(down right). The measured cross section slowly increase as a function of centre-of-mass energy in agreement with the theoretical expectation. At highest LEP energy $\sigma_{Wev} = 0.8$ pb.

Events with one lepton and missing energy in events with at least two jets are produced from W pair production processes when one W boson decays leptonically and the other hadronically.

Events with two leptons and missing transverse energy

This topology is mainly produced by the W pair production process, with subsequest leptonic decay of both W bosons. The rate of such events is sizeable at LEP. In the analysis performed by the OPAL collaboration [17], 416 events are found at highest LEP energies ($\sqrt{s} = 205 \div 209$ GeV) for 423.3 ± 2.5 predicted. In total 1317 events were detected in the highest energy range ($\sqrt{s} = 183 \div 209$ GeV).

The cross section of the W pair production has been measured including also the hadronic decays channels and the combined LEP result is presented in figure 2.5(down left). The increase of the cross section at the kinematical threshold $\sqrt{s} \simeq 2M_W$ is measured. Good agreement with the Standard Model prediction is observed. At highest LEP energy $\sigma_{WW} = 17$ pb.

2.2.4 Events with leptons and photons

Due to the initial state radiation, lower energy beam electrons are produced accompanied by photons colinear with the beam direction. The hard scattering involves either the lower energy electrons (radiative e^+e^- process) or the photon (Compton scattering). The radiative processes scan a large domain in the

[1] The leptons in events with a decay $Z \to \nu\bar{\nu}$ are of opposite sign and same flavour. This process can be used in principle used to measure the Z production, but the improvement of the measurement is tiny due to the modest branching ratios involved. The signature in the electroweak scattering of a $Z \to \nu\bar{\nu}$ decay would be an electron at low energy and nothing else in the detector.

center of mass energy. The Compton scattering $e\gamma \rightarrow e\gamma$ yields events with an electron and a photon at large polar angles and transverse momenta in the final state, while the non-colliding electron is either lost down the beam–pipe or detected close to it. A similar pattern is observed for the non-colliding photon in radiative e^+e^- interactions. The effective center of mass energy $\sqrt{s'}$ is calculated from the detected particles.

The analysis done by the L3 collaboration [18] uses a data sample including center of mass energies from 89 to 180 GeV. After the deconvolution of the photon flux, the Bhabha scattering cross section is measured for an effective cms energy $\sqrt{s'} = 40 \div 180$ GeV. The Compton scattering cross section is measured for $\sqrt{s'} = 15 \div 170$ GeV. Both Bhabha and Compton measurements are found in good agreement with the expectations. Limits on excited electron production and decay $e^* \rightarrow e\gamma$ are obtained.

The final states of four leptons plus a photon has also been studied at LEP [3, 19]. The cross section is dominated by the ISR and therefore the topology of the observed events displays a photon detected close to the beam pipe. The production of $4\ell\gamma$ events where the photon is produced during the main hard scattering is below 1 fb at LEP and therefore undetectable. This final state is suited for the search of anomalous quartic gauge couplings.

Events with one or more photons and missing energy can be produced at LEP through two processes: radiative returns to the Z resonance ($\mathrm{e^+e^-} \rightarrow \gamma\mathrm{Z}$) with Z$\rightarrow \nu\bar{\nu}$, and t-channel W exchange with photon(s) radiated from the beam electrons or the W. The cross section has been measured [20] $\sigma(e^+e^- \rightarrow \nu\bar{\nu}\gamma(\gamma)) = 4.7 \pm 0.8 \pm 0.2$ pb for $\sqrt{s} = 172$ GeV and found consistent with the Standard Model predictions of 4.85 ± 0.04 pb.

2.3 Lepton production in $p\bar{p}$ collisions at Tevatron

The production of leptons is a precious tool for Standard Model tests and new physics searches in $p\bar{p}$ collisions. The hadronic environment implies difficult background conditions for the exclusive final states relying on multi–jet topologies. The enormous QCD jet production is still the main background for the leptonic channels due to the jet misidentification into leptons. This experimental effect is however under control and can be studied with data. Careful energy calibration is required in order to insure the measurement of events with missing energy in the final state.

2.3.1 Events with charged leptons

The production of two charged leptons at Tevatron proceeds mainly through the Drell-Yan mechanism [21]. The neutral current annihilation $q\bar{q} \rightarrow \ell^+\ell^-$ proceeds mainly through the γ^* or the Z boson in the s–channel and gives rise to a pair of opposite charge leptons in the final state[2].

The Z production cross section at $\sqrt{s} = 1.96$ TeV has been measured using the most recent data from Tevatron run 2 : $\sigma(p\bar{p} \rightarrow Z + X \rightarrow e^+e^- + X) = 267 \pm 23$ pb. This measurement is in agreement with the Standard Model prediction of 252.1 ± 8.8 pb that takes into account the NNLO–QCD corrections [23].

The events with high mass $\ell^+\ell^-$ pairs are potential candidates for the physics beyond the Standard Model . The search for such events has been performed on run 1 data [24] and repeated on the recent

[2] The production of a pair of leptons by quark-antiquark annihilation, the Drell-Yan mechanism, can be used to extract information about the proton structure, in particular about the sea quark distribution [22]

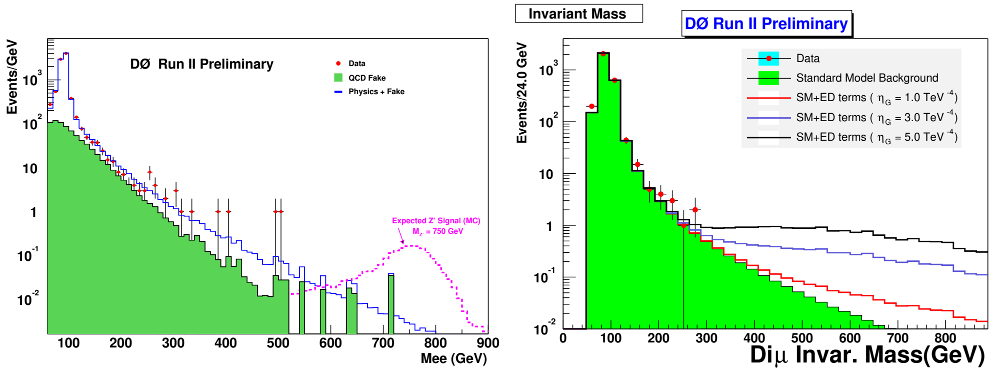

Figure 2.6: The spectra of di-lepton invariant mass obtained in runI by the D0 experiment for electrons(left) and muons(right).

run 2 data. The invariant mass spectra for the di-electron and di-muon channels are shown in figure 2.6. Events with di-lepton invariant masses up to 500 GeV have been measured. The forward backward charge asymmetry can be measured and used to extract information about possible non-standard contribution [25].

2.3.2 Events with charged leptons and missing energy

The search for events with at a lepton and missing transverse momentum has been performed on the run 1 data [26] and recently updated with the new run 2 data. The main Standard Model process that contribute to this final state is the production of W boson through a Drell-Yan annihilation $q\bar{q}' \rightarrow W \rightarrow \ell\nu$. The main quark flavour pairs that produce W's are $u\bar{d} \rightarrow W^+$ and $d\bar{u} \rightarrow W^-$. By measuring the lepton charge asymmetries in the W production useful information is provided for the valence quark flavour composition of the proton [27] .

Events with isolated leptons (electrons or muons) at high transverse momentum $P_T^{\ell} > 25$ GeV and significant transverse energy $P_T^{\text{m}iss} > 25$ GeV are selected. The transverse mass is shown in figure 2.7(left) for an analysis done by the CDF collaboration on run 2 data [28].

The weak boson production is a powerful test of both the electroweak sector of the Standard Model and the proton stucture. The cross sections of the weak boson production in $p\bar{p}$ collisions is shown in figure 2.7(right) as a function of $\sqrt{s}$. The main systematical error is due to the luminosity measurement. The ratio of W to Z production cross sections is insensitive to this error and can be used to extract the W boson width.

The production of two charged leptons in events with missing transverse energy has also been studied at the Tevatron. The signal within the Standard Model is the W pair production. This channel has a potential interest in triple gauge couplings (γWW) and Higgs production at the Tevatron ($H \rightarrow W^+W^-$). In a recent CDF analysis, five candidate events are found against an expected WW signal of 6.89 ± 1.53 events and a background of 2.34 ± 0.38 events in a run 2 data sample with a luminosity of approximately 126 pb^{-1}. The cross section is measured:

$$\sigma_{meas}^{p\bar{p}\rightarrow WW} = 5.1^{+5.4}_{-3.6}\ (\mathrm{stat})\ \pm\ 1.3\ (\mathrm{syst})\ \pm\ 0.3\ (\mathrm{lumi})\ \mathrm{pb}$$

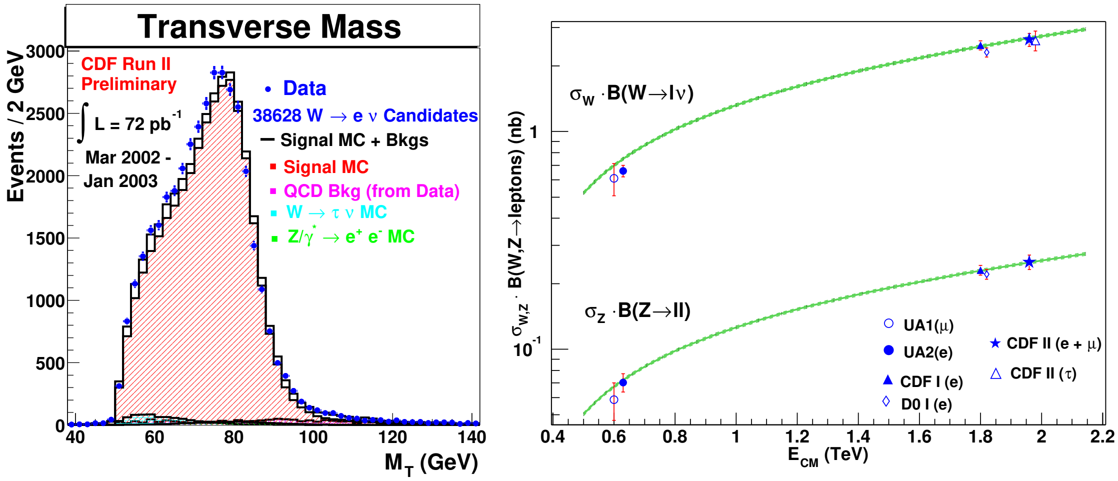

Figure 2.7: Left: the transverse mass distribution of events with isolated leptons and missing transverse energy produced in $p\bar{p}$ collisions at Tevatron RUN II ($\sqrt{s} = 1.96$ TeV). Right: the cross sections of weak boson(s) production in $p\bar{p}$ collisions as a function of $\sqrt{s}$.

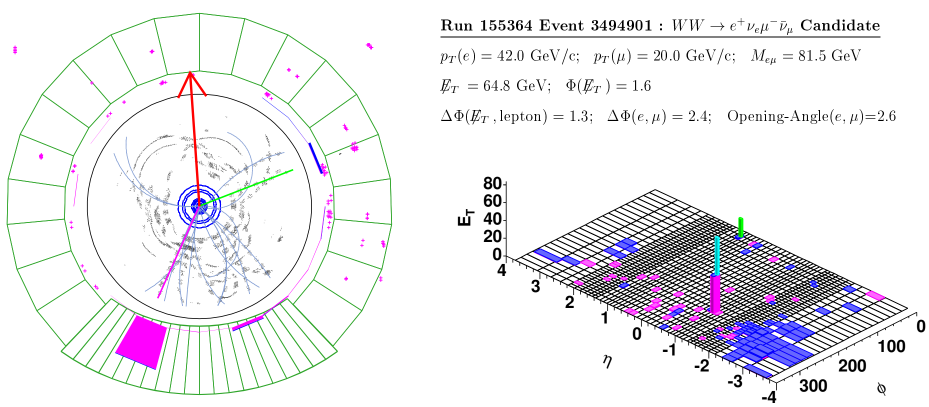

Figure 2.8: A WW candidate in $e\mu + P_T^{miss}$ channel at CDF.

in agreement with the NLO-QCD calculation [29]:

$$\sigma^{p\bar{p}\to WW}_{theo:NLO} = 13.25 \pm 0.25 \text{ pb} .$$

A display of a WW candidate event found in run 2 data with an electron, a muon and missing transverse momentum in shown in figure 2.8.

The production of top quarks can also lead to events with leptons and missing energy in the final state, if one or both of the top quarks decay semileptonically $t \to bW \to bl\nu$. The top candidate events also have at least two jets in the final state. The leptonic channel profits from a small and well understood background and can be used for the measurement of the top mass by a fit to the kinematical distributions [30] of the selected events. In the present run 2 data sample (CDF,$\mathcal{L} = 126\,\text{pb}^{-1}$) at $\sqrt{s} = 1.96$ TeV, a few top candidates have been identified in the semileptonic channel and the production cross section has been measured:

$$\sigma^{p\bar{p}\to t\bar{t}} = 7.3 \pm 3.4(\mathrm{stat.}) \ \pm \ 1.7(\mathrm{syst.})\mathrm{pb} \ .$$

The top quark can also be single produced in association with a b quark through an s-channel W boson splitting or via and W-gluon fusion mechanism [31]. The single top is therefore produced through electroweak mechanisms and the production rate is sensitive to the V_{tb} CKM matrix element. The search for single top production is difficult due to the high background from top pair production [32, 33]. The predicted cross section is around 2 pb and no signal has been found at present. The existing limits of the single top production cross section obtained from the data are typically around 20 pb.

2.4 Lepton production at HERA

In electron-proton collisions, events with high energetic leptons in the final state are mainly produced through the deep inelastic scattering process. In the interaction process, the exchanged virtual boson resolves the quark structure of the proton. In this case the proton can be seen as a flux of quarks. The hard eq interaction may proceed through neutral currents $eq \to eq$ (NC) or charged currents $eq \to \nu q'$ (CC). In the case of a large virtuality (Q^2) of the exchanged boson, the scattered lepton has a large transverse momentum and leads to a prominent experimental signature: an isolated electron in the central detector for NC and significat missing transverse momentum in the case of CC, due to the undetected neutrino.

The CC interaction proceeds only through weak interactions (t-channel exchange of a W boson) and is therefore in general much less intense than the NC process which has the important electromagnetic component (γ^* exchange) together with the weak contribution (Z exchange). Only at very large virtualities $Q^2 \simeq M_{W,Z}^2$ the CC and NC interactions have comparable rates. This can be seen in figure 2.9 where the cross sections for the NC and CC interactions are shown as a function of Q^2 [34]. This figure beautyfully show the electroweak scale unification. At high $Q^2 \simeq M_{W,Z}$, the parity violating couplings play a role and the differences between the cross sections measured in e^+p and e^-p collisions are observed also for NC.

The production of more than one lepton ($\Delta N_L > 0$) in ep collisions is a higher order process with respect to CC/NC processes and appears therefore at a much lower rate. The production mechanisms involve both boson–boson fusion and boson conversion. The production mechanisms within the Standard Model framework together with the experimental observations are described below.

2.4.1 Events with isolated leptons and missing transverse momentum

Standard Model mechanisms

At parton level a lepton-neutrino pair can be produced via the reactions $e^+q \to e^+q'\ell\nu$. The typical Feynman diagrams together with schematic view of the poles are presented in figure 2.10. The dominant contribution is due to the real W boson production and its subsequent leptonic decay, shown in figure 2.10 (a and b). The boson–boson fusion, shown in figure 2.10 (c and d), count for about 5% and yields events with flat distribution of the $\ell\nu$ invariant mass. The CC-like reaction $e^+q \to \overline{\nu}q'\ell\nu$ involves an extra W boson propagator connected to the initial electron in the diagrams and is therefore supressed.

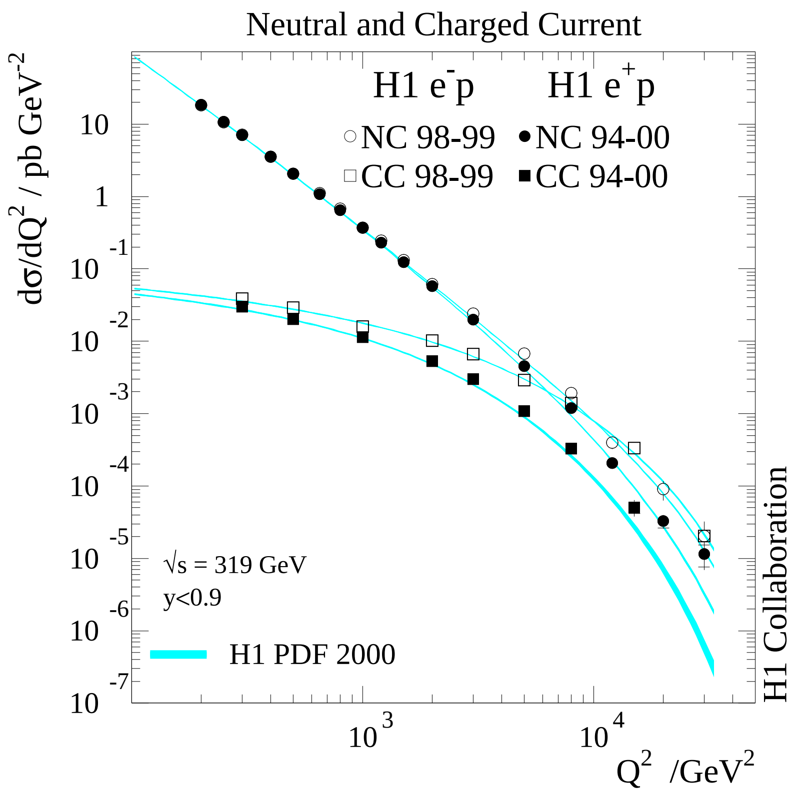

Figure 2.9: The Q^2 dependences of the NC(circles) and CC(squares) cross sections $d\sigma/dQ^2$ shown for the combined 94–00 e^+p (solid points) and 98–99 e^-p (open points) data. The results are compared with the corresponding Standard Model expectations determined from the H1 PDF 2000 fit.

The real W production mainly proceeds through the coupling of the W boson to the quark line, shown in figure 2.10(a). It is dominated by the photoproduction mechanism: the photon entering the reaction from the electron side (figure 2.10(b)) is close to its mass-shell ($Q^2 \simeq 0$) and fluctuates to a $q\bar{q}$ pair. The W boson is then produced in a $q\bar{q}'$ fusion between a quark originating from the photon hadronic fluctuation and another (different flavour) quark from the proton. Interestingly enough, the production mechanism is of hadronic nature: the photon provides the hadronic flux in front of the incoming proton. Due to the $q\bar{q}'$ knock-on nature of the hard scattering, the transverse momenta of the proton or photon rests are typically small and therefore the transverse momentum of the hadronic final state is expected to be close to zero.

In case of large photon virtuality, the W production is a DIS-like scattering with a W-strahlung from the quark line. In this case the scattered electron is visible in the detector together with the charged lepton issued from the W decay. This is the case for 25% of the simulated events in H1 detector. In this configuration, the hadronic system X can also acquire important transverse momentum.

The production of a $\ell - \nu$ pair in boson–boson ($\gamma - W$ or $Z - W$) collision is sketched in the diagrams c) and d) in figure 2.10. This non-resonant production contributes to less than 5% to the total cross section. The W boson can also be produced by a triple boson coupling $WW\gamma$, by the $\gamma - W$ fusion. HERA sensitivity to an anomalous coupling will be discussed in the next chapter.

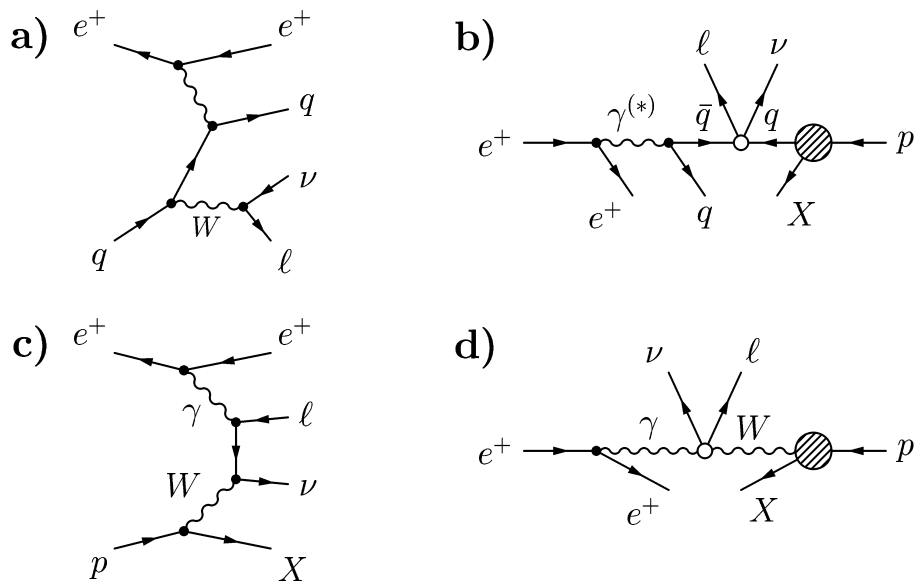

Figure 2.10: The schematic view of the lepton-neutrino production in ep collisions. The real W boson production as radiation from the quark line (a) is mainly produced in photon-production process sketched in diagram (b). The non-resonant $\ell\nu$ pair can also be produced in a t-channel fermion exchange between two boson $\gamma - W$. This corresponds to a boson-boson fusion sketched in (d). A similar mechanism yields real W bosons through triple boson couplings $WW\gamma$.

The first complete calculation of W production in ep collisions has been done in [35]. An event generator (EPVEC) has been used to interface the calculation to the full detector simulation. The EPVEC generator includes the QCD parton shower simulation in the final state [36].

The SM prediction for W production via $ep \to eW^{\pm}X$ is calculated by using a next to leading order (NLO) Quantum Chromodynamics (QCD) calculation [37] in the framework of the EPVEC [35] event generator. Each event generated by EPVEC according to its default LO cross section is weighted by a factor dependent on the transverse momentum and rapidity of the W [38], such that the resulting cross section corresponds to the NLO calculation.

The NLO corrections are found to be of the order of 30% at low W transverse momentum (resolved photon interactions) and typically 10% at high W transverse momentum (direct photon interactions) [37, 39, 40]. The NLO calculation reduces the theory error to 15% (from 30% at leading order).

The charged current process $ep \to \nu W^{\pm}X$ is calculated with EPVEC [35] and found to contribute less than 7% of the predicted signal cross section.

The total predicted W production cross section amounts to 1.1 pb for an electron–proton centre of mass energy of $\sqrt{s} = 300$ GeV and 1.3 pb for $\sqrt{s} = 318$ GeV.

Another possible contribution to the signal in the electron channel only is the production of the Z boson with the subsequent decay to neutrinos: $ep \to eZX \to e\nu\bar{\nu}X$. In this case the isolated lepton is the “scattered” electron. This process is also calculated in EPVEC. The main contribution at large transverse momenta is not from the photoproduction mechanism, for which the scattered electron tend to be rather backward[3], but the Cabibbo-Parisi process, induced by a fluctuation of a photon from the proton into an e^+e^- pair, with the annihilation of one of those electron with the beam positron to produce the Z boson[4]. The contribution of this process to the cross section is around 3%.

First observations

The observation of events with isolated leptons and missing transverse momentum has been made first at HERA back in 1994. In a sample of CC events with a transverse momentum in the calorimeter P_T^{calo} above 25 GeV, a spectacular event with an isolated muon in the final state has been observed [41]. The event was detected in a data sample corresponding to an integrated luminosity of 4 pb^{-1}. The sum of the expected contributions from the Standard Model processes was estimated to be 0.03 events.

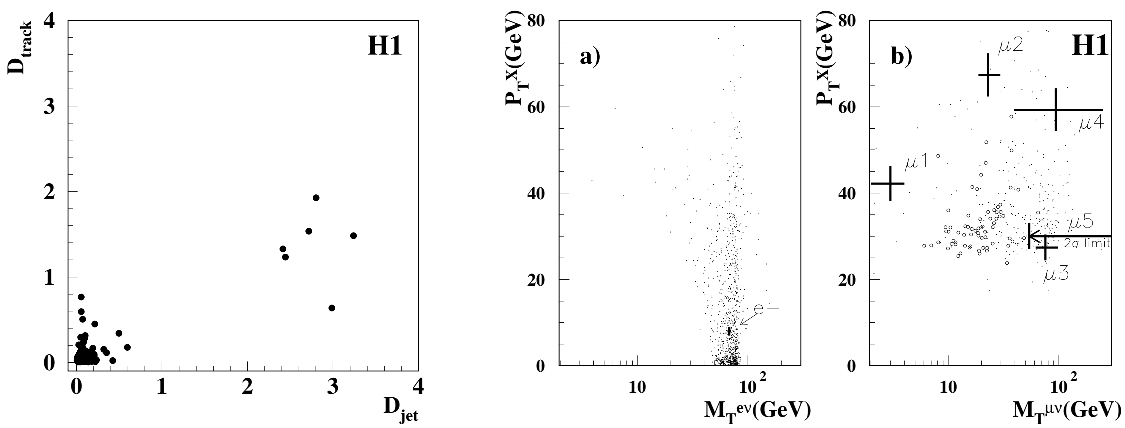

Figure 2.11: Early observations of events with isolated leptons and missing transverse momentum by H1. Left: correlation between the distances D_{jet} and D_{track} to the closest hadronic jet and track, for all high-P_T tracks in the inclusive event sample. Right: distribution of the selected events in P_T^X and $M_T^{l\nu}$ (see text): a) electron channel; b) muon channel.

The analysis of a data sample collected in the period 1994-1997 in e^+p collisions corresponding to an integrated luminosity of 37 pb^{-1} was performed for the phase space with large imbalance in the calorimetric transverse momentum $P_T^{calo} > 25$ GeV [42]. The isolation of the charged tracks with large transverse momenta $P_T^{track} > 10$ GeV was calculated in each event with respect to the closest track (D_{track}) and with respect to the closest hadronic jet (D_{jet}). Figure 2.11 shows the correlation between D_{track} and D_{jet} for the high-P_T tracks in the inclusive event sample. In most cases the high-P_T tracks are not isolated. This is expected, since the bulk of events are CC interactions with the high-P_T track located within or close to the hadronic shower. However, six high-P_T tracks are found in a region well separated from all other charged tracks and from hadron jets. They belong to six events each with one single isolated high-P_T charged particle. All six isolated high-P_T particles fulfill the lepton identification criteria. One is an electron candidate and five are muon candidates.

[3]The origin of the coordinate system at HERA experiments is the nominal ep interaction point. The direction of the proton beam defines the positive z–axis (forward direction).

[4]see also next section for the explanation of this mechanism

The total yield of events with one isolated high-P_T lepton which is expected from SM processes is 2.4 ± 0.5 in the $e^{\pm}$ channel and 0.8 ± 0.2 in the $\mu^{\pm}$ channel. The main contribution is due to W production, estimated in leading order to be 1.7 ± 0.5 and 0.5 ± 0.1 events respectively.

The kinematics of the observed events is compared to the Standard Model prediction in figure 2.11. Shown is the distribution of the events in the hadronic transverse momentum P_T^X and the transverse mass [5] plane. The electron event and one of the muon events are found in a region of phase space likely to be populated by W production. Another muon event can, within its large measurement errors, also be accommodated in a W interpretation. The kinematic properties of the remaining three muon events, together with the overall rate excess in the muon channel, disfavour an interpretation of these events within the SM processes considered.

Events with $\ell + P_T^{\mathrm{miss}}$ in HERA I data

The search for events with isolated leptons and missing transverse momentum has been performed on the full HERA I dataset. The H1 analysis [43] has been extended at lower transverse momentum $P_T^{calo} > 12$ GeV in order to increase the acceptance for the real W boson production. The leptons with transverse momenta above 10 GeV are identified in the polar angle domain $5^\circ < \theta < 140^\circ$ using also the detection capabilities in the forward region. The background rejection is inforced [44] in order to cope with the huge cross sections of the photoproduction, NC and CC processes.

The ZEUS analysis of the full HERA I data [45] specifically searches for events with isolated leptons and missing transverse momentum having also a hadronic system at large transverse momentum. The analysis is done in the framework of the seach for anomalous top production. Events with significant calorimetric imbalance are selected with $P_T^{calo} > 20GeV$. In each such event, the leptons are identified as isolated tracks with transverse momenta above 5 GeV in the polar angle range $17^\circ < \theta < 115^\circ$. The tracks are required to be associated with specific calorimetric patterns for electrons or muons.

A search for events with isolated tau's at HERA has been recently published by ZEUS collaboration [46]. In this case the isolated track is required to correspond to a calorimetric deposit compatible with a narrow jet with small track multiplicity produced by a hadronic tau decay. The discrimination of the tau signal from the quark induced jets is done by using a multivariate analysis based on six variables related to the shape of the calorimetric deposit. The analysis of the H1 data in the τ channel is currently in progress.

The results of the search for isolated leptons with missing transverse momentum at HERA is summarized in table 2.1 and figure 2.12. The data is compared with the Standard Model expectation for the full HERA I period. The phase space region at large hadronic transverse momentum is also shown. The H1 analysis has better non-W background rejection at low and high transverse momentum.

With a more powerfull background rejection and an extended phase space at lower transverse momentum [44], the H1 analysis provide clear evidence for the single W boson production at HERA. The cross section measured at low and high hadronic transverse momentum is shown in table 2.4.1. It is compared to the LO and NLO predictions and found in good agreement at low P_T^X and slightly in excess (about 2σ) at high P_T^X.

[5] The transverse mass is calculated from the massless four vectors obtained by projecting the missing and the lepton momenta on the plane transverse to the beams direction: $M_T^{\ell\nu} = \sqrt{(P_T^{miss} + P_T^{\ell})^2 - (\vec{P}_T^{miss} + \vec{P}_T^{\ell})^2}$

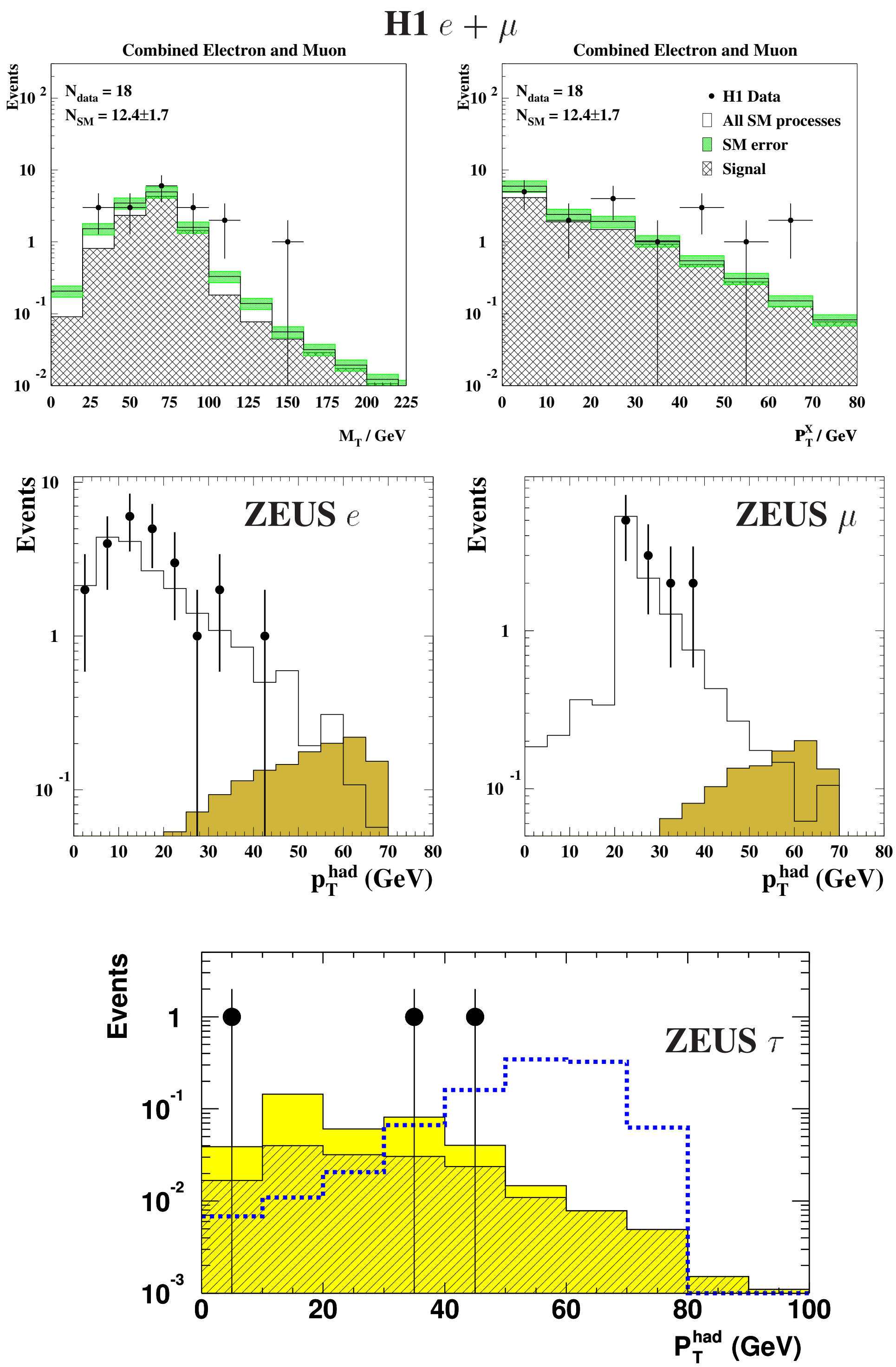

Figure 2.12: The kinematical distribution of events with isolated leptons and missing P_T for H1 and ZEUS analysis. (the shaded (e and μ plots) and the dashed (τ) histograms in ZEUS plots represent the distributions of the single-top MC normalised to an integral of one event).

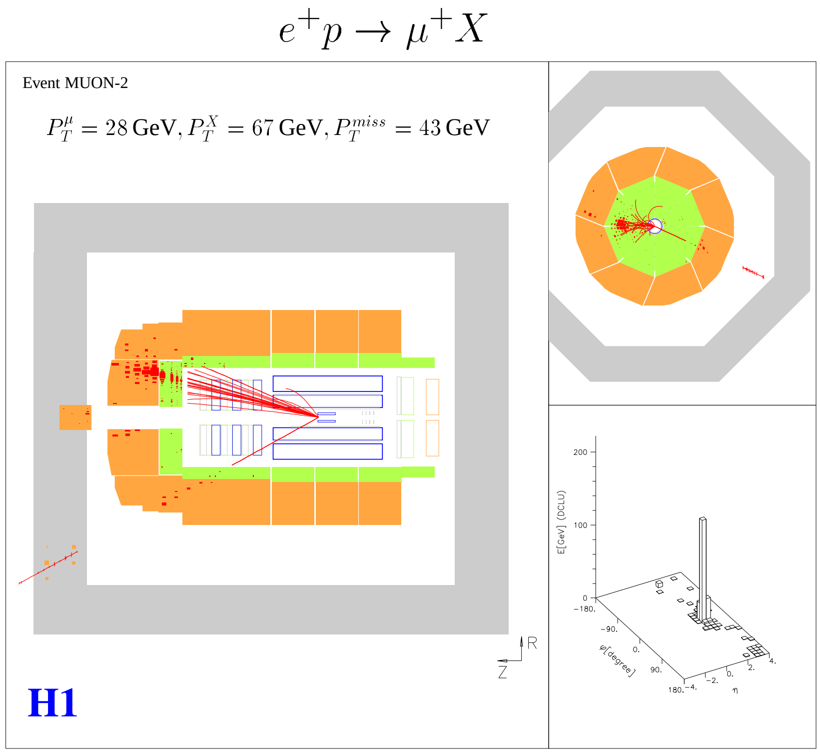

Figure 2.13: Display of an event with an isolated muon, missing transverse momentum and a prominent hadronic system. The acoplanarity between the lepton and the hadronic system is the signature of an undetected particle.

Both experiments observe events with isolated leptons and missing transverse energy. Good agreement is found with the expectation from the Standard Model in the phase space at low hadronic transverse momentum $P_T^X < 25$ GeV. An excess is observed by the H1 analysis at large trasverse momentum $P_T^X > 25$ GeV. One such event is from the H1 analysis is shown in figure 2.13. The probability of the Standard Model expectation to fluctuate above the observed number of events is 10% for the full sample and 0.15% at $P_T^X > 25$ GeV. The ZEUS analysis does not find such a prominent excess in the electron and muon channels, but observes tau events with large P_T^X. In total at HERA I, in the region $P_T^X > 25$ GeV, 20 events with isolated leptons are observed for a total expectation of roughly 9.3 ± 1.8. The HERA II data, with an increase of a factor of ten in the integrated luminosity, will help in the clarification of this observation[6].

2.4.2 Events with several charged leptons

The main SM processes involved in multi–electron production at HERA are summarized in figure 2.14.

The dominant contribution is the interaction of two photons radiated from the incident electron and proton, also called Bethe-Heitler (BH) contribution and shown in diagram 2.14a. The kinematical pole

[6]The quantification of the excess based on the statistical CL_b method applied to the P_T^X spectrum can be found in [47]. Some possible scenarios of the excess and a discussion of the compatibility between H1 and ZEUS observations are studied in [48, 49].

1994-2000 $e^{\pm}p$		Electron obs./exp. ($W^{\pm}$ contribution)	Muon obs./exp. ($W^{\pm}$ contribution)	Tau obs./exp. ($W^{\pm}$ contribution)
H1	Full sample	11 / 11.54 ± 1.50 (71%)	8 / 2.94 ± 0.50 (86%)	
	$p_T^{\rm had} > 25$GeV	5 / 1.76 ± 0.30 (82%)	6 / 1.68 ± 0.30 (88%)	
118.4 pb^{-1}	$p_T^{\rm had} > 40$GeV	3 / 0.66 ± 0.13 (80%)	3 / 0.64 ± 0.14 (92%)	
ZEUS	Full sample	24 / 20.6 $^{+1.7}_{-4.6}$ (17%)	12 / 11.9 $^{+0.6}_{-0.7}$ (16%)	3 / 0.40 $^{+0.12}_{-0.13}$ (49%)
	$p_T^{\rm had} > 25$GeV	2 / 2.90 $^{+0.59}_{-0.32}$ (45%)	5 / 2.75 $^{+0.21}_{-0.21}$ (50%)	2 / 0.20 $^{+0.05}_{-0.05}$ (49%)
130.2 pb^{-1}	$p_T^{\rm had} > 40$GeV	0 / 0.94 $^{+0.11}_{-0.10}$ (61%)	0 / 0.95 $^{+0.14}_{-0.10}$ (61%)	1 / 0.07 $^{+0.02}_{-0.02}$ (71%)

Table 2.1: Summary of the results of searches for events with isolated leptons, missing transverse momentum and large $p_T^{\rm had}$ at HERA. The number of observed events is compared to the SM prediction. The $W^{\pm}$ component is given in parentheses in percent. The statistical and systematic uncertainties added in quadrature are also indicated.

	Cross Section / pb			
	Measured	SM NLO	SM LO Diener *et al.*	SM LO Baur *et al.*
$P_T^X < 25$ GeV	0.146 $\pm$ 0.081 $\pm$ 0.022	0.194 $\pm$ 0.029	0.147 $\pm$ 0.044	0.197 $\pm$ 0.059
$P_T^X > 25$ GeV	0.164 $\pm$ 0.054 $\pm$ 0.023	0.043 $\pm$ 0.007	0.041 $\pm$ 0.012	0.049 $\pm$ 0.015

Table 2.2: The measured cross section for events with an isolated high energy electron or muon with missing transverse momentum (H1 collaboration). The cross sections are calculated in the kinematic region: $5° < \theta_l < 140°$; $P_T^l > 10$ GeV; $P_T^{\rm miss} > 12$ GeV and $D_{jet} > 1.0$. Also shown are the signal expectations from the Standard Model where the dominant contribution $ep \to eWX$ is calculated at next to leading order (SM NLO) [37, 38] and at leading order (SM LO) [37] and [35].

corresponds to a two photons collision sketched in figure 2.14b. The hadronic final state (X) can be a proton (elastic process), a proton resonance (quasi–elastic process) or a high mass system in case of high virtuality of the photon from the proton side (inelastic process).

The produced electron pair can also originate from a γ^*/Z boson, radiated either from the electron line (diagram 2.14c) or from the quark line (diagram 2.14e). This process, also called internal conversion, has two kinematical poles. First, the Cabibbo–Parisi (CP) process, sketched in figure 2.14d), involves an e^+e^- interaction where one of the electrons is issued from a photon radiated from the proton[7]. Its contribution is one order of magnitude lower than the photon-photon contribution, except at high transverse

[7] Pairs of leptons for which the kinematics do not correspond to the $\gamma\gamma$ collisions have first been observed in e^+e^- collisions at ADONE and interpreted as an underlying e^+e^- annihilation by Cabibbo and Parisi in a private communication to the experimentalists [50, 51]

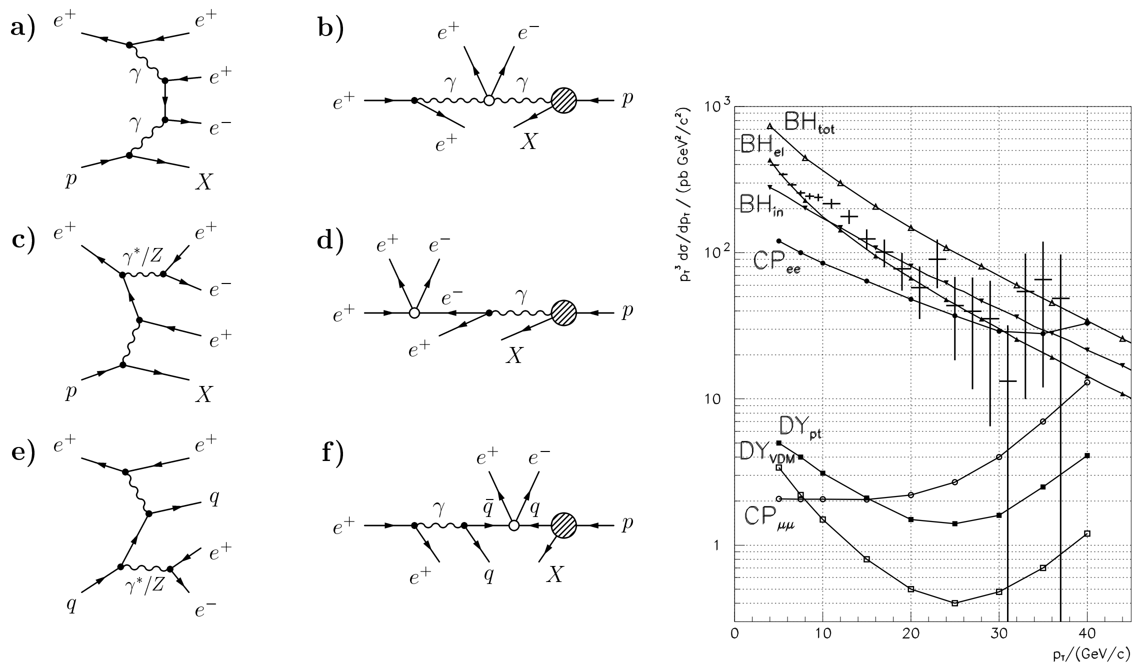

Figure 2.14: Main processes involved in lepton pair production (left and middle) and their cross sections(right). Example of Feynman diagrams (left) for a): photon–photon interaction; c) and e): γ^*/Z boson conversion. The kinematical poles for basic $2 \to 2$ lepton pair production processes are sketched (middle) for b): photon–photon collisions $\gamma\gamma \to e^+e^-$; d): Cabibbo-Parisi $e^+e^- \to e^+e^-$; f): Drell-Yan $q\bar{q} \to e^+e^-$.

momentum where it contributes more significantly due to the s-channel Z boson contribution. The second pole of internal conversions is the Drell–Yan (DY) process (figure 2.14f), involving a quark–antiquark interaction where the anti-quark (close to its mass shell) is issued from a photon radiated from the incident electron [8]. Its contribution is small compared to photon-photon and Cabibbo-Parisi processes [54].

The contribution of different processes can be seen in figure 2.14 (right) [55] where the differential cross section multiplied by the cube of the electron transverse momentum is shown as a function of electron P_T. The increase of the CP and DY contributions in the region of $P_T \simeq M_Z/2$ is due to the contribution of the Z propagator in s-channel for those processes. The multi–electron production at HERA has been first computed in the photon-photon mode in [56] and implemented in the LPAIR generator [57]. The full matrix element calculation, except for the Drell-Yan pole, is done in [58] and implemented in the GRAPE generator which is used for signal simulation. The background is composed from NC events with a second fake electron from the hadronic final state and from Compton scattering $ep \to e\gamma X$ where the photon is wrongly identified as the second electron in the event.

Measurement of multi-electron events

Both H1 and ZEUS experiments at HERA have measured multi-lepton production at high transverse momenta [59, 60, 61].

[8] The contribution from Drell-Yan process has been proposed as an interesting probe of proton or photon structure at HERA [52, 53].

Selection	DATA	SM	GRAPE	NC-DIS + Compton
H1 115 pb^{-1}	$20° < \theta^{e1,2} < 150°$, $P_T^{e1} > 10$ GeV, $P_T^{e2} > 5$ GeV			
“2e”	108	117.1 ± 8.6	91.4 ± 6.9	25.7 ± 5.2
“3e”	17	20.3 ± 2.1	20.2 ± 2.1	0.1 ± 0.1
“2e” $M_{12} > 100$ GeV	3	0.30 ± 0.04	0.21 ± 0.03	0.09 ± 0.02
“3e” $M_{12} > 100$ GeV	3	0.23 ± 0.04	0.23 ± 0.03	< 0.02 (95% C.L.)
ZEUS 130 pb^{-1}	$17° < \theta^{e1,2} < 167°$, $P_T^{e1} > 10$ GeV, $E^{e2} > 10$ GeV			
“2e”	191	213.9 ± 3.9	182.2 ± 1.2	31.7 ± 3.7
“3e”	26	34.7 ± 0.5	34.7 ± 0.5	–
“2e” $M_{12} > 100$ GeV	2	0.77 ± 0.08	0.47 ± 0.05	0.30 ± 0.07
“3e” $M_{12} > 100$ GeV	0	0.37 ± 0.04	0.37 ± 0.04	–

Table 2.3: Observed and predicted multi-electron event rates for masses $M_{12} > 100$ GeV as function of the number of identified electrons. The prediction errors for H1 analysis include model uncertainties and experimental systematical errors added in quadrature. For ZEUS analysis, the predicted rates are shown with the statistical errors of the Monte Carlo only.

The electron identification is based on calorimetric information inforced by tracking conditions for efficient background rejection. Electrons are measured in a large acceptance range $5° < \theta_e < 175°$, where θ_e is the electron polar angle measured with respect to the incoming proton direction. The electron energy measured from calorimetric information has to be above 5 GeV. This energy threshold is inforced in H1 (ZEUS) analysis to 10 GeV for electrons candidates with $\theta_e < 20°$ ($\theta_e < 164°$). The electron candidates have to be isolated from other calorimetric deposits. In the central region defined by $20° < \theta_e < 150°$ for the H1 analysis and $17° < \theta_e < 164°$ for the ZEUS analysis, an isolated charged track measured in the central tracking system has to be associated to the calorimetric deposit. The identified electrons are indexed in decreasing transverse momentum P_T: $P_T^{e_i} > P_T^{e_{i+1}}$.

The selection of multi-electron events is based on the requirement of two central electrons with high energy or transverse momentum. Both the H1 and ZEUS analyses require the first central electron to have the transverse momentum above 10 GeV. The second central electron is required to have $P_T^{e2} > 5$ GeV ($E^{e2} > 10$ GeV) in H1 (ZEUS) analysis. Any other electron identified is also counted and the selected events are classified by the number of identified electrons in the event.

The results of the H1 and ZEUS analyses are presented in table 2.3. The H1 analysis, based on an event sample corresponding to 115 pb^{-1}, measured 125 multi-electron events, while ZEUS, with an integrated luminosity of 130 pb^{-1}, detected 217 such events. The di-electron sample is dominated by the signal with a 15-20% contribution from the background. In the tri-electron sample, the background contribution is negligible. Both H1 and ZEUS observations are in good agreement with the predicted rates. The main difference between the H1 and ZEUS acceptances for the signal is due to a different angular range for the central electrons.

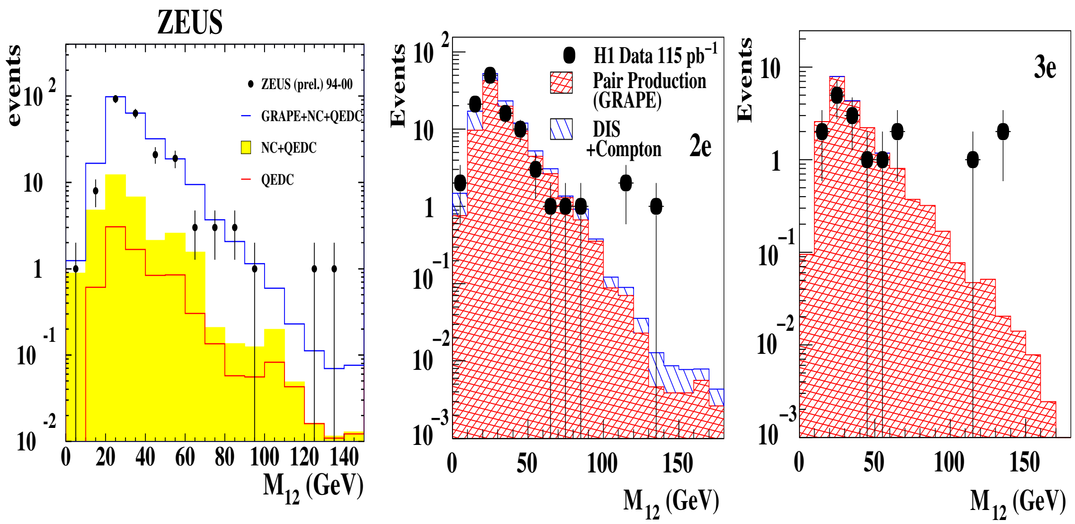

Figure 2.15: Distribution of the invariant mass M_{12} of the two highest P_T electrons for the the ZEUS analysis (left). All observed events with two electrons or more are shown. Distribution of the invariant mass M_{12} of the two highest P_T electrons for the H1 analysis (center and right). Events are classified as di-electrons (center) and tri-electrons (right).

The distributions of the invariant mass of the two highest P_T electrons are shown in figure 2.15. Data is in good overall agreement with the Standard Model prediction. A few events with masses $M_{12} > 100$ GeV are observed in a region where the standard model prediction is low. H1 measured 3 di-electron events for 0.30 expected. ZEUS observed 2 di-electron events for 0.77 expected. In the tri-electron sample, H1 observed 3 events with $M_{12} > 100$ GeV for an expectation of 0.23 while ZEUS do not observe events in that mass region for an expectation of 0.37. For the high mass di-electron events, the transverse momenta of the two electrons is also important (above 50 GeV). The topology of the observed tri-electron high-mass events is different: the transverse momenta of the two highest P_T electrons is lower (around 30 GeV) and the high mass value is associated with a larger polar opening angle between the two electrons (“forward-backward” topology). One di-electron and one tri-electron at high mass are shown in figure 2.16.

Alltogether, at high mass $M_{12} > 100$ GeV, H1 and ZEUS observe 8 multi–electron events for an expectation of 1.67 ± 0.20. A possible interpretation of the observed multi-electron events in terms of doubly charged higgs production at HERA is presented in the next chapter.

Measurement of multi-muon events

Muons are identified using central tracker, calorimeter and muon chambers signals. Search for multi-muon events has been performed by H1 [60] and ZEUS [61].

The H1 collaboration measures the di-muon production for muons with $P_T > 2$ GeV in the angular range $20^\circ < \theta < 160^\circ$. Figure 2.17 (left) presents the visible cross section measured by H1 [60] as a function of the invariant mass of the muon pair compared to the Standard Model prediction. Backgrounds and also other sources of muon pair production like heavy hadron decays are negligible. Very good agreement with Standard Model prediction is observed up to the highest masses and over a decrease of

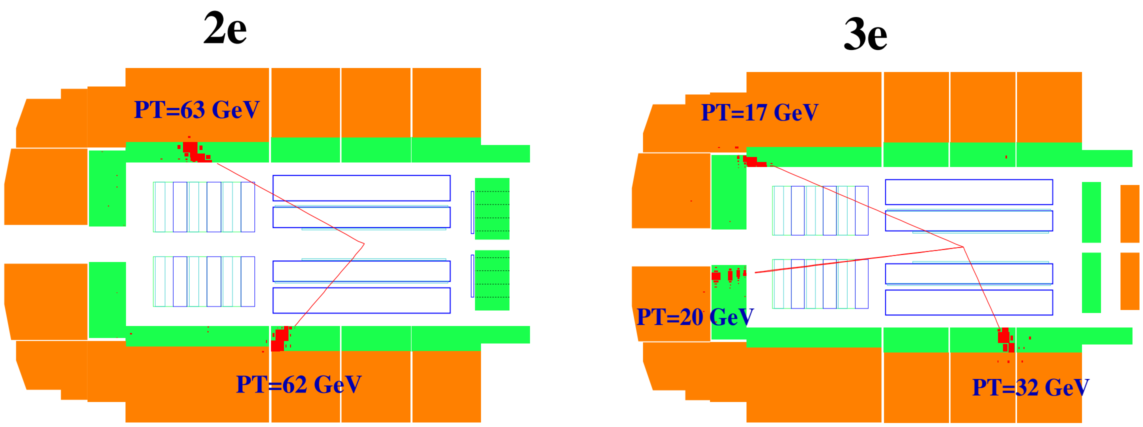

Figure 2.16: Event displays of two of the H1 multi-electron candidates: a di-electron (left) with large electron transverse momentum and a tri-electron (right) at lower P_T with forward-backward topology of the highest P_T electron pair that form M_{12}.

four orders of magnitude. The integrated cross section in the visible phase space has been measured to 46.5 ± 4.7 pb which is in good agreement with the prediction of 46.2 pb.

A search for multi-lepton events ($\ell\mu\mu$) at high P_T has been performed by requiring at least two muons in the region $20° < \theta < 150°$ with transverse momenta $P_t^{\mu_1} > 10$ GeV and $P_t^{\mu_2} > 5$ GeV. Additional muons must be detected in the central region of the detector, $20° < \theta_\mu < 160°$, with a minimum transverse momentum of 1.75 GeV. Additional electrons are searched for in the polar angle range $5° < \theta_e < 175°$ and are required to have a minimum energy of 5 GeV. With this selection 56 di-muon events are found, among which 16 events have an extra identified electron ($\mu\mu e$ events). In figure 2.17 (center) the di-muon mass distributions of events classified as $\mu\mu$ events or as $\mu\mu e$ events are compared with the theoretical expectations. Both mass distributions are in agreement with the Standard Model calculations. The distribution in M_{12}, the invariant mass of the two leptons with the largest P_t, is shown for the $\mu\mu e$ sample in figure 2.17 (right). This mass combination is selected in order to compare with the H1 multi-electron analysis, where the scattered electron cannot be identified uniquely. For approximately half of these events, the two leptons with the highest P_T are the electron and a muon. For these events, the mass distribution $M_{12}^{\mu e}$ is also shown in figure 2.17 (right).

For masses $M_{12} > 100$ GeV (> 80 GeV) one $\mu\mu$ event is found, while 0.08 ± 0.01 (0.29 ± 0.03) are expected. This inelastic event with two well identified muons has a mass of $M_{\mu\mu} = 102 \pm 11$ GeV. No event classified as $\mu\mu e$ with $M_{12} > 100$ GeV is observed. The prediction is 0.05 ± 0.01. These results at high di-lepton masses are in agreement with the Standard Model predictions. In view of the present limited statistics, they cannot be used to draw firm conclusions concerning the high mass excess observed in the multi-electron analysis.

In the ZEUS analysis two muons with $P_T^{\mu 1,2} > 5$ GeV in the angular range $20° < \theta < 160°$ are required. With an analyzed data sample corresponding to an integrated luminosity of 105 pb^{-1}, ZEUS detects 200 events for an expectation of 213$\pm 11_{stat}$. No event with two muons at high mass $M_{\mu\mu} > 100$ GeV is observed.

It should be noted that the detection of the muon as a “third” lepton is presently done for a polar angle $\theta > 20°$, while the electrons are detected in a more forward region $\theta > 5°$. It is important to extend

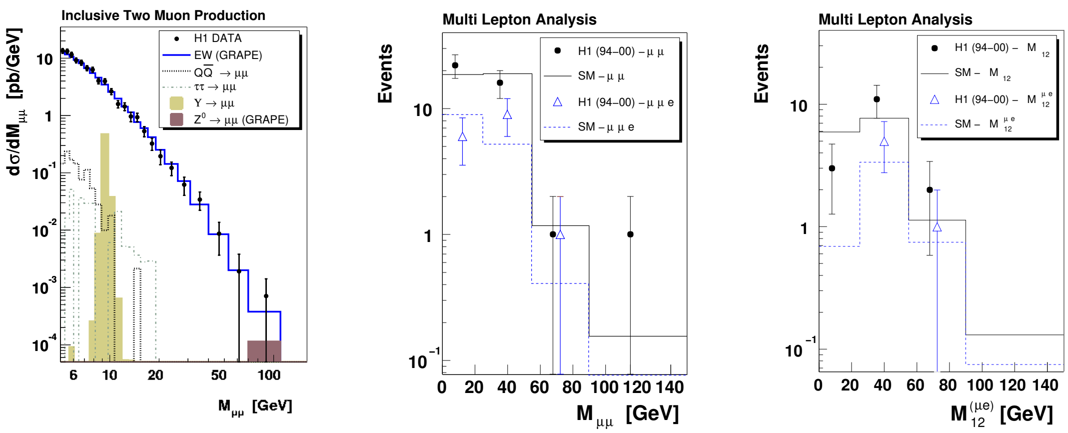

Figure 2.17: Muon pair production cross section as a function of the invariant di-muon mass (left). Distributions of the invariant mass $M_{\mu\mu}$ for compared with the Standard Model predictions (right). Distribution of $\mu\mu e$ events as function of mass M_{12} of the two highest P_t leptons, and of the mass $M_{12}^{\mu e}$ for those events where the leptons with the highest P_t are a muon and the electron.

in future the search for muons at a lower polar angle because high mass states tend to be boosted in the forward direction (at low polar angles) at HERA.

In the case of a multi–electron final state, there exists the possibility that the "scattered" electron is a part of the highest P_T electron pair and that one of the "produced" electrons is lost down the beam pipe. This is expected to be the case for half of the di-electron events at high masses ($M > 100$ GeV), as predicted by the GRAPE generator [58] . The full cross check of the production of multi-lepton events with muons should include the $e\mu$ final states in the future.

3 Isolated Leptons as Signals Beyond the Standard Model

3.1 Welcome to BSM-land!

What is usually called “physics beyond the Standard Model” (BSM) is a part of the unknown. The theories not yet positively confirmed or falsified by the experimental data (including the mechanism of symmetry breaking of the Standard Model) have an equal probablity to be true.

At colliders, high P_T lepton production is a signal easy to measure. The processes producing leptons in the final state span a large range of Standard Model tests, as has been illustrated in the previous chapter. The events with high energy leptons also provide gold plated channels for the observation of the new physics beyond the Standard Model.

There are many patterns in which the theories extending the Standard Model are classified. The most extensive ones define problems of the Standard Model and classify the models according to the solutions to those problems. There are theories that would like to save the Standard Model from family replication, from fine tunning, from leptons and quarks non-symmetry, from neutrinos being too light or from the top quark being too heavy. It might well be that some assumption or the theory as a whole is part of the NSM (next Standard Model). Only new experimental data can solve the puzzle.

Here we adopt a sequential scheme to classify the models of the new physics, according to the proximity of the new phenomena to the final state leptons. The idea is that, if some signal above the background show up in the data, the source of the deviation can be localized at various levels during the evolution from the initial state to the final state. This is illustrated in figure 3.1. The particle production is represented as a tree where the new (BSM) mechanism modifies one of the vertices during the hard interaction process:

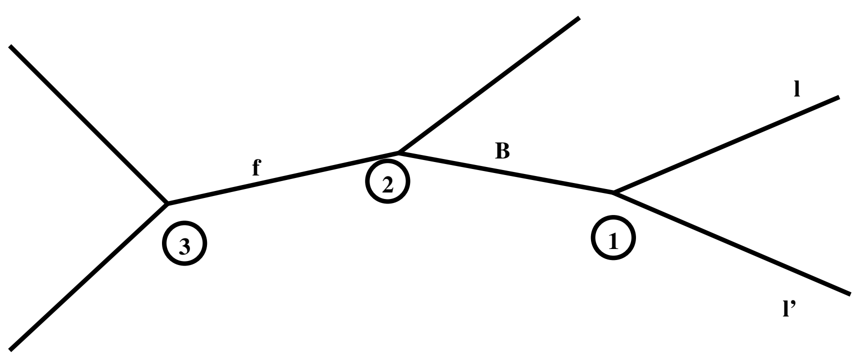

Figure 3.1: Lepton production in a fermion-boson-leptons cascade. The anomaly beyond the Standard Model may occur in lepton (1), boson (2) or fermion (3) production couplings (see text).

1. The lepton couplings are modified. This is the case if the leptons are produced by a new scalar or vector boson (H^{++}, W', Z').

2. The vector bosons of the Standard Model are anomalously produced by tri-boson anomalous couplings or in the decays of new fermions, for instance the excited fermions.

3. A special case in the Standard Model is the top quark, the only fermion that decays into real W bosons. The source of anomalies in the lepton production may also be traced back to an anomalous top production.

Examples related to these patterns for physics beyond the Standard Model are discussed in this chapter.

3.2 Anomalous lepton production

Anomalous production of leptons at high transverse momenta can be predicted by theories that incorporate new symmetries and new bosons decaying to Standard Model leptons. The most constrained BSM theory is the Standard Model itself for the scalar sector, not yet measured experimentally. However couplings are predicted to be proportional to the mass and little impact from the direct Higgs decay to leptons is expected.

New scalar and vector bosons are proposed in models that extend the Standard Model, like the Left-Right Symmetric, supersymmetric, GUT models or combinations of those [62]. Examples of searches for such new bosons are described below.

3.2.1 New charged and neutral vector bosons

The search for extra gauge boson production (W', Z') in $p\bar{p}$ collisions at the Tevatron is done using the leptonic decay channel. The hadronic decay channel has little sensitivity due to the large QCD background.

The search for a neutral Z' boson is based on the detection of two charged leptons (electrons or muons). The main Standard Model contribution is due to the Drell-Yan process, as mentioned in the previous chapter. The searched signal is a peak in the di-lepton invariant mass spectrum. No such peak has been detected up to now and the data is in good agreement with the expectation from the Standard Model up to the highest observed masses, as mentioned in the previous chapter (figure 2.6). An asymmetry in the angular distribution for high mass lepton pairs can also be a sign of a new boson and can be used for instance to investigate the indirect effects of a compositeness model [25]. Limits on the production of Z' are obtained by combining the electron and muon channels. Neutral boson masses are excluded at 95% confidence level for masses below an upper limit in the range between 545 and 730 GeV, depending on the models.

A search for an extra charged gauge boson W' is performed in events with leptons and missing energy. In the analysis done by CDF on run I data [26] assuming the strength of the Standard Model coupling, the W' mass limit is set to be $M(W') > 755$ GeV at the 95% confidence level.

The Tevatron sensitivity to extra gauge bosons decaying to SM leptons should finally reach about 1 TeV in run 2, while $4 \div 5$ TeV should be accessible at the LHC [28].

3.2.2 Doubly charged higgs H^{++}

The Left-Right (LR) symmetric models [63, 64, 65] provide some interesting features like the see-saw mechanism that explains the smallness of the neutrino mass together with the non-observation of right handed currents. The LR Standard Model extensions of the Standard Model predict higgs boson triplets containing doubly charged Higgs H^{++}. Due to the charge, they can only couple to leptons. This is an example of a BSM process that affects only the leptonic sector [62]. Since the Higgs triplet is not related to the symmetry breaking mechanism, the coupling is not necessarily proportional to the mass and can therefore be large also in the case of electrons and muons. The mechanisms of H^{++} production at colliders are shown in the diagrams of figure 3.2.

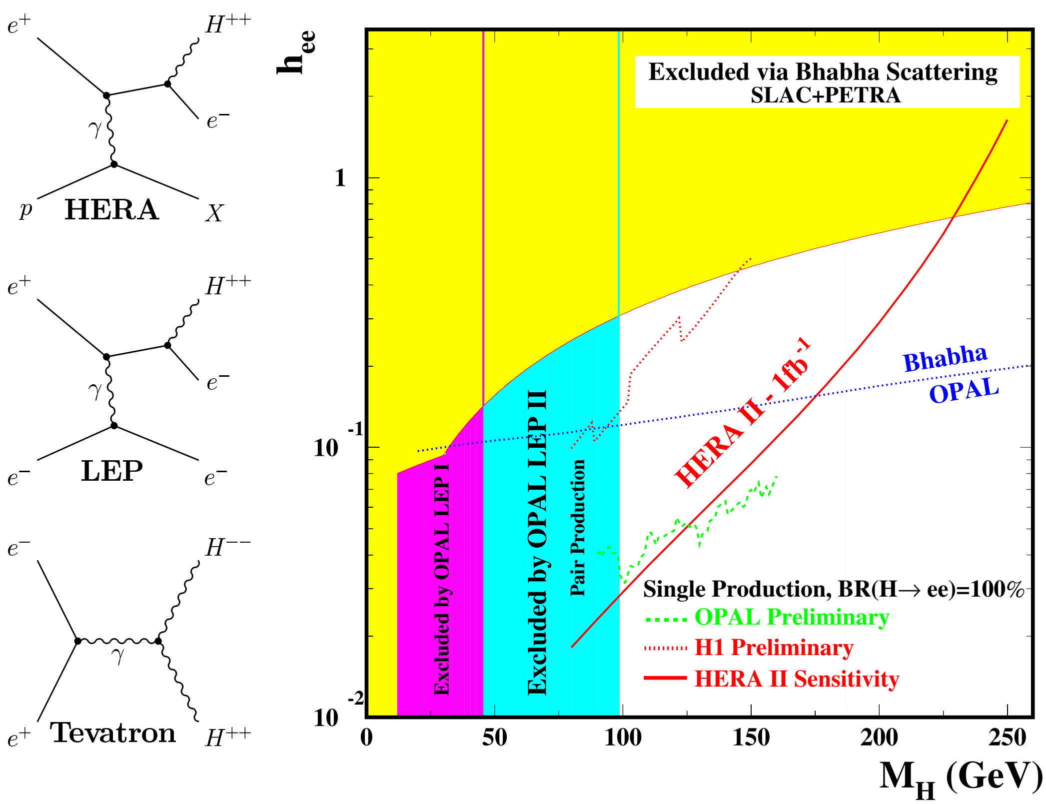

Figure 3.2: Mechanisms involving doubly charged higgs at colliders (left) and world status of the limits on the coupling to electrons h_{ee} versus Higgs mass. The previsions for next running period at HERA II is also indicated.

Doubly charged higgs particles can be pair produced at the Tevatron through a Drell-Yan mechanism $e^+e^- \rightarrow H^{++}H^{--}$. The final state consists of four charged leptons and has little background. The production cross section is independent of the H^{++} couplings. At the Tevatron the search for resonances in a sample of events with four electrons or two electrons and two muons has started for Run II data [28]. A sensitivity up to $M_{h^{\pm\pm}} \simeq 180$ GeV is forseen for the full run II data taking. The pair production mechanism has also been studied at LEP [66]. No deviation with respect to the Standard Model has been found and a lower limit on the H^{++} mass of about 100 GeV has been derived at 95% confidence level, independent of the couplings.

At HERA, single $H^{\pm\pm}$ can be produced in a hard $e\gamma^{(*)}$ scattering. The final state consists of two or three charged leptons which may make the H^{++} production an attractive interpretation of the high mass multi-electron events observed at HERA and discussed in the previous chapter. But this is not the case since among the six events with two or three electrons at high mass only one remains consistent with the H^{++} interpretation [67].

The single H^{++} production is also possible at LEP [68] through a mechanism very similar to HERA. The final state consists of two or three leptons, searched for in an flavour independent analysis. The main Standard Model backgrounds are the fermion pair production and the production of events with four leptons. The requirement that same-sign leptons form the higgs candidate at high mass reduces the background typically by a factor of 10-20 in the final stage of the analysis. The final sample consists of 55 events, in rough agreement with the Standard Model expectation of 44 ± 2. The events are uniformely distributed in invariant mass from 80 GeV up to roughly 150 GeV. In contrast, in the H1 analysis, the Standard Model expectation falls steeply with the invariant mass. However, the larger luminosity of LEP ensures a better sensitivity for H^{++} searches.

At LEP, the doubly charged Higgs boson can modify the Bhabha scattering cross section due to the exchange in the t-channel. The Bhabha cross section has been measured and found in very good agreement with the Standard Model prediction. Indirect limits on the doubly charged higgs model parameters (mass and couplings) can be obtained.

The status of H^{++} searches is shown in figure 3.2. The exclusion limit at 95% confidence level on the couplings to electrons h_{ee} is shown as a function of the H^{++} mass.

3.2.3 Bileptons

New bosons can also be studied in a more general framework of bileptons [69], bosons that couple to leptons but not to quarks. A special case are the bileptons for which the leptonic number $L = 2$ which explicitely prevents the boson coupling to quarks.

Simply charged bileptons $L^{\pm}$, coupling to a lepton-neutrino pair, can be produced by pairs at LEP or Tevatron and yield final state topologies with two leptons and missing transverse momentum, similar to the W–pairs in the case in which both W bosons decay in the leptonic channel[1]. At HERA, single $L^{\pm}$ can be produced in $e\gamma$ collisions ($e^+\gamma \to \nu L^+$) and yield final state topology similar to the W production process discussed in the previous chapter. The hadronic system is expected to have low transverse momentum and an important fraction of the production cross section should belong to the elastic process, for which the proton is left unbroken and no hadrons are observed in the main detector. This makes unlikely the interpretation of the outstanding $\ell + P_T^{miss}$ events as bilepton $L^{\pm}$ production. The single charged bileptons can also be simply produced at LEP in $e\gamma$ collisions, with a similar final state as the single W production in case of the W leptonic decay. This production channel should provide a sensitivity to bileptons with mass up to the available $\sqrt{s}$ at LEP.

The doubly charged bileptons can also be produced by pairs at LEP and Tevatron and singly at LEP and HERA. The production of doubly charged bileptons can yield final states with multi-leptons, particularly interesting in view of the observed multi–lepton events at HERA. The case of the doubly charged

[1] The search for charged Higgs pairs can also be interpreted in terms of searches for bilepton pairs if the hadronic decays are ignored. In the ALEPH analysis [70], a lepton-flavour blind search for tau decays a limit for the production cross section around 0.8 pb^{-1}, assuming 100% branching ratio to $\tau\bar{\nu_\tau}$. However the rejection of the W–pairs relies on the charged higgs model. Supposing the effect of the signal modelling is small, this analysis can also be used to extract a limit on the bilepton pair production at LEP.

higgs presented above gives an idea about the relative sensitivities. However, it would be interesting to perform a complete analysis of the "hadro-phobic" boson production at LEP, HERA and Tevatron in the framework defined in [69].

3.3 Anomalous EW boson production

The lepton production through the Standard Model weak bosons can present anomalies if those bosons result from new particle decays. Two examples are given here.

3.3.1 Excited fermions

An anomalous production of weak bosons can result from the radiative decay of higher mass excited states of the known fermions. Excited fermions represent a natural scenario for the compositeness extensions of the Standard Model. The production and decay of excited fermions are described in terms of the phenomenological Lagrangian proposed in [71].

$$L_{ff^*} = \frac{e}{\Lambda} \sum_{V}^{\gamma,Z,W} \bar{F^*} \sigma^{\mu\nu} (c_V - d_V \gamma^5) F \partial_\mu V_\nu + h.c. \tag{3.1}$$

where c_V and d_V are coupling constants at the fermion $F \leftrightarrow F^*$ vertex labelled for each vector boson V, and Λ is the compositeness scale. The precise measurement of muon $g-2$ and the absence of an electron or muon electric dipole moments implies that $c_V = d_V$ for compositeness scales less than 10–100 TeV. This fact leads to an interaction Lagrangian where the coupling constants of excited fermions to Standard Model gauge bosons are described in terms of three constants corresponding to the three gauge groups: f for $SU(2)_L$, f' for $SU(1)_Y$ and f_s for $SU(3)_C$. For specific assumptions relating f, f' and f_s the branching ratios can be predicted and the cross sections are described by a single parameter (e.g. f/Λ).

The search for excited fermions is performed at all colliders by searching for fermion-boson resonances. As an example, the mechanisms of excited electron production are shown in figure 3.3 (left). Although the branching to a photon is favoured in the majority of parameter configurations, the coupling to the photon can vanish in some cases. For instance the $\nu^*\nu\gamma$ coupling tends to zero for $f = f'$. In this case the decay $\nu^* \to \nu\gamma$ is forbidden and the search for ν^* must rely on final states with weak bosons [72]. Similarly, the decay $e^* \to e\gamma$ is forbidden for $f = -f'$ and the excited electron decays only in eZ channel [73].

No signal for radiative decays of a high mass fermion has been found. The limits on coupling normalized on the compositeness scale (f/Λ) are calculated. The present status for the excited electron e^* is shown in figure 3.3. LEP excludes, with high sensitivity to the coupling, excited electrons with masses up to $\sqrt{s}$. Beyond that, HERA experiments, for which the e^* production proceeds with photons from the proton, provide sensitivity for masses up to 250 GeV but for couplings ten times larger than at LEP. The production at Tevatron has less sesitivity for low couplings but it may directly probe excited fermion masses well beyond HERA or LEP. For the next running period, HERA will have the priviledged discovery window at low couplings and for masses in the range between 200 and 300 GeV.

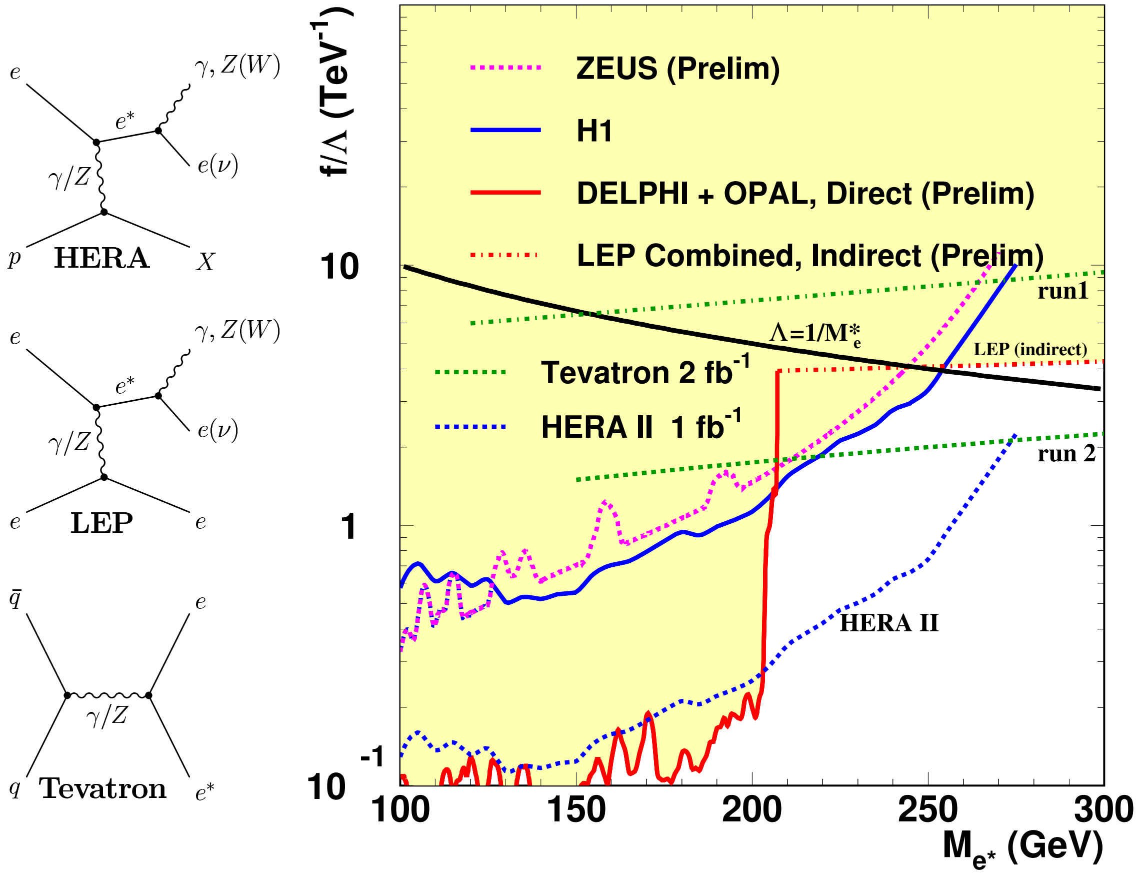

Figure 3.3: Mechanisms of excited electron production at colliders (left) and the 95% confidence limits of the coupling normalized to the compositeness scale as a function of the excited electron mass (right, figure from [28]). Previsions for next running periods at HERA and Tevatron are also indicated.

3.3.2 Gauge bosons anomalously coupled

The Standard Model of particle physics is a non-Abelian theory and therefore predicts that the gauge bosons interact with each other, allowing coupling vertices such as WWZ and $WW\gamma$. The trilinear couplings can be measured experimentally. For instance, the flattening of the $e^+e^- \rightarrow W^+W^-$ cross section with $\sqrt{s}$ (figure 2.5) is the experimental proof of the existence of the tri-linear coupling [74, 75] that damps the linear increase of the cross section predicted by the W pair production mechanism provided by a neutrino exchange in the t-channel. The value of the couplings may be modified by radiative corrections involving particles predicted by extensions to the Standard Model such as Supersymmetry. Models based on substructure of the gauge bosons would also lead to non Standard Model or "anomalous" couplings. Making experimental measurements of the couplings is therefore an important test of the Standard Model and its extensions.

The most general Lorentz invariant Lagrangian which describes the triple gauge boson interaction has fourteen independent complex couplings, seven describing the WWγ vertex and seven describing the WWZ vertex [76]. Assuming electromagnetic gauge invariance as well as C and P conservation, the number of independent TGCs reduces to five. A common set is $\{g_1^Z, \kappa_Z, \kappa_\gamma, \lambda_Z, \lambda_\gamma\}$ where $g_1^Z = \kappa_Z =$

$\kappa_\gamma = 1$ and $\lambda_Z = \lambda_\gamma = 0$ in the Standard Model . The parameters proposed used by the LEP experiments are g_1^Z, λ_γ and κ_γ with the gauge constraints:

$$\kappa_Z = g_1^Z - (\kappa_\gamma - 1)\tan^2\theta_W\,, \quad (3.2)$$
$$\lambda_Z = \lambda_\gamma\,, \quad (3.3)$$

where θ_W is the weak mixing angle. The couplings are considered as real, with the imaginary parts fixed to zero.

Note that the photonic couplings λ_γ and κ_γ are related to the magnetic and electric properties of the W-boson. One can write the lowest order terms for a multipole expansion describing the W-γ interaction as a function of λ_γ and κ_γ. For the magnetic dipole moment μ_W and the electric quadrupole moment q_W one obtains $e(1+\kappa_\gamma+\lambda_\gamma)/2m_W$ and $-e(\kappa_\gamma-\lambda_\gamma)/m_W^2$, respectively.

Parameter (95% C.L.)	Standard Model	LEP	Tevatron (D0 - run I)	HERA (40 pb^{-1})
κ_γ	1.0	$[0.835,\ 1.052]$	$[0.02,\ 2.01]$	$[-3.7,\ 2.5]$
λ_γ	0.0	$[-0.067,\ 0.028]$	$[-0.33,\ 0.31]$	$[-3.2,\ 3.2]$

Table 3.1: The 95% C.L. intervals obtained combining the results from the four LEP experiments and from the D0 and ZEUS analyses. In each case the parameter listed is varied while the other two are fixed to their Standard Model values.

The measurement of triple gauge couplings has been performed at LEP. For instance, in the analysis [77, 78] done by ALEPH collaboration, the $WW\gamma$ vertex is investigated in events with single photons, single W bosons or W pairs. No deviations from the Standard Model are found. The triple gauge couplings are tested at Tevatron in the di-boson production, for instance in the D0 analysis of the run 1 data [79]. The best sensitivity is obtained in the $W\gamma$ channel where limits on the deviations of the couplings from their Standard Model values are obtained. At HERA, the single production of W bosons can in principle also be used to set limits on the anomalous triple gauge couplings. HERA sensitivity to an anomalous coupling has been investigated by the ZEUS collaboration [80].

The 95% confidence intervals from the three colliders are presented in table 3.1. Deviations from the Standard Model with $\lambda \neq 0$ or $\Delta\kappa = \kappa - 1$ may lead to a production of $\ell + P_T^{miss}$ events with atypical kinematical properties at HERA [81]. However, HERA sensitivity is significantly smaller than that of LEP or the Tevatron to this type of anomalus couplings and therefore the interpretation of the events with isolated leptons and missing transverse energy as W production through an anomalous triple gauge coupling is largely disfavoured.

3.4 Anomalous top production

Due to the large top quark mass close to the electroweak scale, phenomena related to the top quark may have the best sensitivity to new physics phenomena. The top quark is only produced at Tevatron, mostly in pairs. LEP and HERA colliders provide sufficient centre-of-mass energy for a single top production in ee and ep collision, respectively. However, the top production cross section within the Standard Model is very low of about 1 fb at HERA [82, 83] and 10^{-4} fb at LEP [84].

Single top search 1994-2000 $e^{\pm}p$	Electron obs./exp. (top efficiency)	Muon obs./exp. (top efficiency)	Hadrons obs./exp. (top efficiency)
H1 118.4 pb^{-1}	$3/0.65 \pm 0.10$ (36%)	$2/0.66 \pm 0.12$ (38%)	$18/20.2 \pm 3.6 (30\%)$
ZEUS 130.2 pb^{-1}	$0/0.94\ ^{+0.11}_{-0.10}$ (35%)	$0/0.95\ ^{+0.14}_{-0.10}$ (35%)	$14/17.6^{+1.8}_{-1.2}$ (25%)

Table 3.2: Summary of the results of searches for anomalous top production in electron, muon and hadronic channels at HERA. The number of observed events is compared to the SM prediction. The efficiency to detect top quark decays in the specified channels is given in parentheses in percent.

The top quark could be produced at HERA and LEP if flavour changing neutral currents were allowed in the top sector [85]. The production mechanisms would be based on the non-vanishing couplings of the top quarks to the light quarks of same charge (up and charm) and to the neutral bosons (γ, Z). In this case, the production of single top quarks at LEP and HERA would proceed through the mechanisms sketched in the diagrams of figure 3.4. In addition, anomalous top quark decays to neutral bosons should be observed in the top sample produced at the Tevatron. The process is usually described[2] using the anomalous couplings $\kappa_{\gamma qt}$ (magnetic coupling to the photon) and v_{Zqt} (vector coupling to the Z) with $q = u, c$.

The search for anomalous decays ($t \to q\gamma$ and $t \to qZ$) of the top quark has been performed at Tevatron [87]. Top pairs are searched for in events for in which one top quark decays via the dominating Standard Model mode $t \to bW$ (the branching ratio is 100% in the Standard Model) and the second via FCNC decays. Two candidate events are found in this search: one event in the mode $t \to qZ$ for which 1.2 events are expected, the second event in the mode $t \to q\gamma$ for which the background is not calculated. Conservative limits are derived by assuming that the observed events belong to the signal. The 95% confidence level limits on the branching fractions are:

$$B^{t\to q\gamma} < 3.2\% \qquad B^{t\to Z\gamma} < 33\%$$

The branching fractions for FCNC decays are proportional to the square of the anomalous couplings [88]. Therefore upper limits on the anomalous FCNC couplings can be calculated. The limits related to the photon and Z are independent. The flavour of the final state is not tagged and the limits apply to both $tu\gamma$ or $tc\gamma$ couplings.

At LEP, the FCNC couplings may lead to associated top-charm or top-up production in a e^+e^- annihilation via a γ^*/Z. The FCNC single top production depends on the couplings to u and c quarks, that is four types of couplings: $tu\gamma, tc\gamma, tuZ$ and tcZ. The main dependence is proportional with the square of the couplings, with some small intererence effect. The events are searched with a top candidate recoiling against a hadronic jet [89, 90, 91]. Limits on the single top production cross section are obtained in the range $0.2 \div 0.7$ pb at various centre-of-mass energies.

If single top quarks are produced at HERA, the experimental signature of the leptonic decays channel $t \to bW \to b\ell\nu$ corresponds to events with isolated leptons, missing transverse energy and a prominent

[2] For a complete langrangian with FCNC in the top sector see for example [85, 86]

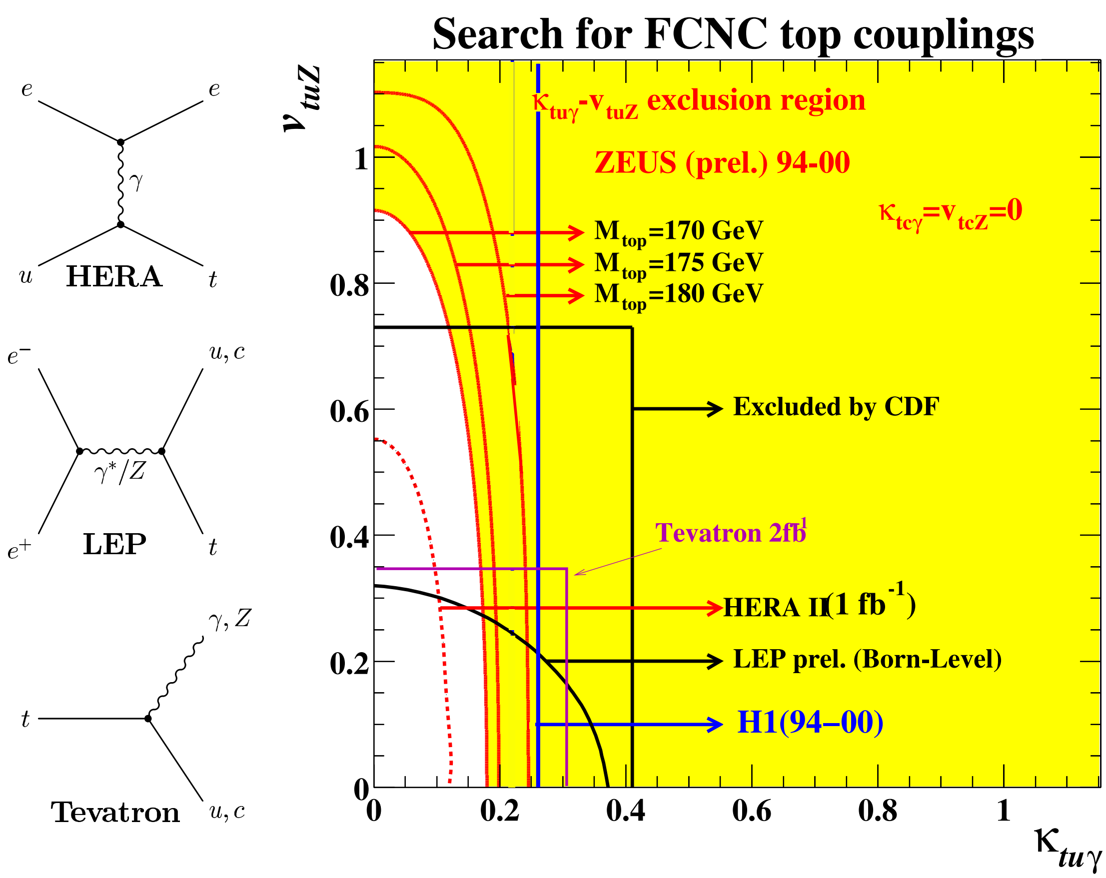

Figure 3.4: Mechanisms involving FCNC top couplings at colliders (left) and world status of the limits on the $tu\gamma$ and tuZ couplings. Previsions for next running periods at HERA and Tevatron are also indicated.

jet. This is particularly interesting in view of the excess of events of this type observed by H1 and discussed in the previous chapter. For the hadronic channel, the signature is three or more jets with high transverse momenta. The search for anomalous top production at HERA is summarized in table 3.2 (H1 [86] and ZEUS [45]). In the H1 analysis, a part of the events with isolated leptons, missing energy and a prominent hadronic jet are also found as top candidates in the electron and muon channels: 5 events for an expectation of 1.3 ± 0.2. In the hadronic channel the sensitivity is much reduced due to the high background originating from QCD multi-jet production.

The limits at 95% confidence level on the anomalous couplings $\kappa_{\gamma ut}$ and v_{Zut} obtained at LEP, Tevatron and HERA are shown in figure 3.4. The sensitivity to the Z couplings has been studied by the ZEUS collaboration and found to have a non-negligible impact at large values of v_{Zut}, a region however already excluded by LEP and Tevatron.

In order to extract the top quark production cross section, a multivariate likelihood analysis is performed by H1 in addition to the cut–based analyses. The top signal contribution in each channel is determined in a maximum–likelihood fit to the likelihood discriminator distributions. The results from the hadronic channel do not rule out a single top interpretation of the candidates observed in the electron and muon channels. For the combination of the electron, muon and hadronic channels a cross section for single top production of $\sigma = 0.29^{+0.15}_{-0.14}$ pb at $\sqrt{s} = 319$ GeV is obtained. This corresponds to a magnetic coupling $\kappa_{tu\gamma}$ of $0.20^{+0.05}_{-0.06}$. This result is not in contradiction with limits obtained by other experiments. The addition of a contribution from a model of anomalous single top production yields a better description of the data than is obtained with the Standard Model alone. The new data at HERA II will allow the improvement the sensitivity to the anomalous magnetic coupling $\kappa_{tu\gamma}$ by roughly a factor of two. For the FCNC coupling to the Z boson, a gain in sensitivity beyond the present LEP limit is expected from the Tevatron run 2 data.

3.5 Supersymmetry

The scheme presented in the beggining of this chapter (figure 3.1) is of course not a theory, but rather a pretext to discuss the path to new physics interpretation, once some deviation from the Standard Model is found in the experimental data. A popular theory that extends the Standard Model is the supersymmetry (SUSY). SUSY provides the unification of internal symmetries with the Lorentz invariance and associates supersymmetric particles ($s$particles) to the known Standard Model particles. The supersymmetric models propose solutions to most of the Standard Model problems (hierarchy, fine–tunning, unification) and predict spectacular final states to be obtained in particle collisions. Despite extensive studies at colliders and elsewhere, no trace of SUSY has been detected yet.

As an example of the capabilities of the SUSY theories to predict spectacular topologies, we shortly present here several hypothesis, some of them not yet fully explored with the present data, that may explain the production of events with high P_T leptons at HERA. The production of single $s$particles is possible at colliders if the multiplicative quantum number R_p is violated (for a particle, the R–parity is $R_p = (-\mathbf{1})^{3B+L+2S}$ where B is the baryon number, L the lepton number and S the spin). For instance, the violation of the R–parity opens the possibility of squark production in the s–channel at HERA due to the electron-quark-squark Yukawa coupling. A special case is the stop ($\tilde{t}$) which in most SUSY scenarios is the lightest SUSY particle.

The produced squarks can decay to eq or νq trough R_p–violating coupling producing events with the same topology as the deep inelastic scattering process. However, gauge decays into a quark and a chargino or a neutralino may lead to complex final state topologies, including configurations with high energy leptons.

There are a few possibilities to produce events with isolated leptons and missing transverse momentum in squark decays at HERA[3]:

- If the squark decay via gauge decays $\tilde{q} \rightarrow q\chi^+$, the semi-leptonic decay of the chargino into a neutralino $\chi^+ \rightarrow \chi^- \ell\nu$ issue an isolated leptons and missing energy together with a large P_T jet from the primary squark decay. If the neutralino is stable, it can travel undetected the apparatus and induce extra missing momentum. The same topology is obtained in the case of the decay chain $\tilde{q} \rightarrow q\chi^+ \rightarrow q\nu\tilde{l}$. If the slepton is stable, then it can fake a muon signature in the detector. However, a stable neutralino or a stable slepton require a SUSY parameter space that is already severely constrained from LEP analyses.

[3] In most scenarios the charge of the prominent isolated lepton in the event correspond to the lepton beam charge

- If in the same configuration as above the neutralino can decay via a R_p violating coupling: $\chi^0 \rightarrow eq\bar{q}$ or $\chi^0 \rightarrow \nu q\bar{q}$. This will give rise to events with either several jets or several charged leptons in the final state. Searches of squark production at HERA by the H1 collaboration have not detected any deviation from the Standard Model prediction [92, 93] and constrained the squark masses up to 290 GeV. The H1 events with isolated leptons and missing transverse energy do not correspond to the predicted topology in the SUSY parameter space, mostly because no multi–jet shape of the hadronic system is observed.

- If we consider the resonant production of stop quarks at HERA, a SUSY parameter space can be considered where the stop is heavier than the sbottom. If in addition the charginos are heavier than the stop, the following channel may have an important contribution to the stop quark decay $\tilde{t} \rightarrow \tilde{b}W$ with subsequent R_p violating decay $\tilde{b} \rightarrow d\nu$. This decays chain produce events with isolated leptons and missing energy accompanied by a prominent hadronic system if $W \rightarrow \ell\nu$ or events with three jets and missing P_T in the case of hadronic W decays. In addition, the R_p violating decays $\tilde{t} \rightarrow eq$ are also present and provide a cross–check of the stop production at HERA in this scenario.

- In the case of two non–zero R–parity violating couplings, the slepton produced in chargino decay can undergo a leptonic decay via a λ coupling: $\chi^+ \rightarrow \tilde{\ell}^+\nu \rightarrow \ell^+\nu\nu$. A large number of final states should be observed at HERA in e^+p collisions [94, 95] (j denotes a hadronic jet):

$$e^+p \rightarrow \tilde{t} \rightarrow \tilde{\chi}_1^+ b \rightarrow \ell^+ j\nu\nu \ , \ \ \ell^+\ell^+\ell^- j \ , \ \ \ell^+ jjj \ , \ \ jjj\nu$$

$$e^+p \rightarrow \tilde{c} \rightarrow \tilde{\chi}_1^0 c \rightarrow \ell^+\ell^- j\nu \ , \ \ \ell^\pm jjj \ , \ \ jjj\nu$$

  Events with an isolated lepton, missing P_T and prominent hadronic system are predicted to appear in conjunction with tri-lepton events and a jet. The compatibility of this hypothesis with the observation of both the $\ell + P_T^{miss}$ events and the multi-lepton events at high mass has to be investigated[4].

SUSY processes may also produce events with several energetic charged leptons. For instance, the production of scalar neutrino [96] via a R_P violating coupling in the leptonic sector (λ), $e^+p \rightarrow \mu^+\tilde{\nu_\tau}X \rightarrow \mu^+\mu^-e^+X$. The signal should produce a peak in the invariant $e^+\mu^-$ mass distribution. If tau leptons are produced in the final state (trough a different λ coupling, $e^+p \rightarrow \tau^+\tilde{\nu_\tau}X \rightarrow \tau^+\tau^-e^+X$), events with narrow jets and missing transverse momentum should be observed.

The supersymmetry can be at the origin of the outstanding events with leptons observed at HERA, altough the most popular scenarios are not likely. A rich phenomenology, with numerous decays channels - typical for the R_p violating SUSY - provides a cross check of this hypothesis and invites for further detailed analyses.

3.6 The model independent new physics search

The data can also be investigated in an model independent approach in order to search for deviations from the Standard Model predictions. The general search for new phenomena has been pioneered by the

[4] No significant missing P_T has been detected in those events. Only one among the six H1 multi-electron events at high mass have a clear hadronic system.

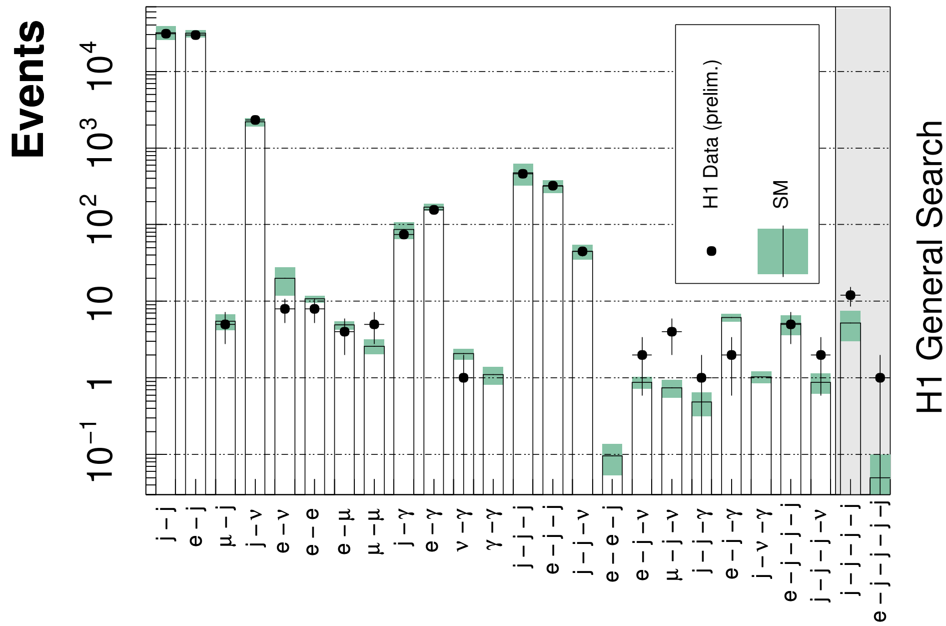

Figure 3.5: The reasult of the H1 general search. The data ((points) and Standard Model expectation (histogram) for all event classes with a SM expectation greater than 0.1 events are shown.

D0 collaboration [97]. The idea is to define a common phase space for all types of final state identified particles. The events are then classified according to the particle content. Kinematical quantities are defined, like the mass and the scalar transverse momentum, and a non-biased search algorithm is applied in order to look for local deviations that may appear due to for instance to a hypothetical multi–channel decay of a heavy particle.

The analysis has also been performed by the H1 collaboration [98]. ‘Objects” are defined from particle identification: electron (e), muon (μ), photon (γ), jet (j) and neutrino (ν) (or non-interacting particles). All final states are analysed having at least two objects with a transverse momentum (P_T) above 20 GeV and in the polar angle range $10^\circ < \theta < 140^\circ$. All selected events are then classified into exclusive event classes (e.g. ej, jj, $j\nu$) according to the number and types of objects detected in the final state. The event samples selected in the different classes are shown in figure 3.5. A very good agreement is found for nearly all those topologies which is a great achievement, taking into account the complexity of the final states that are studied. The data fluctuate over the Standard Model in the $\mu j\nu$, as expected from the previous observations. The statistical analysis of the mass and P_T spectra also identifies the observed fluctuation in the multi–electron channel, no visible on the global rate of ee channel shown in figure 3.5. No other significant deviation with respect to the Standard Model has been found in addition.

The general search at high P_T gives a global view of the physics rates as a function of the final state topology and require a good understanding of the Standard Model and of the detector. This type of analysis is necessary for the searches program at present and future colliders, as it provides an extra security belt against the unexpected phenomena that may occur in a new pattern, different from what is predicted from the existing models.

4 Conclusion

The detection of isolated leptons at large transverse momenta at colliders provides an unique tool for the study of the processes involving the basic structure of the matter. The present colliders LEP (e^+e^- collisions), HERA (ep collisions) and Tevatron ($p\bar{p}$) collisions are complementary and span a wide range of hard scaterring processes.

Within the Standard Model framework, the lepton production proceeds either through boson splitting or via boson–boson scattering. The investigation of the final states with isolated leptons allows to test the electroweak sector of the Standard Model . The production of weak bosons, single or by pair, at LEP and the Tevatron is found in agreement with the precise calculations based on the Standard Model. The boson production at HERA is a rather rare process and the production of the W boson has been experimentally demonstrated. The observation of a few spectacular events with isolated leptons, missing transverse momentum and a prominent hadronic jet is puzzling and needs more integrated luminosity to be clarified. The measurement of the production of events with several charged leptons is particularly interesting at HERA and the Tevatron due to the particular conditions of production: QED processes coupled to the intimate structure of the protons entering the reaction. The study of the spectacular multi-electron events with high masses observed in the HERA I data will continue at HERA II with large statistics.

The search for new physics is particularly interesting in the leptonic channels due to usually low and theoretically well understood rates of the Standard Model processes. The search for new phenomena suppose that "something" may start to deviate from the Standard Model laws at lepton couplings, vector boson couplings or top quark couplings. The examples given in this paper shed light on the complementarity between the three colliders for the search of the new physics beyond the Standard Model.

The forthcoming years will bring an increased data sample at HERA and the Tevatron, comparable with the excellent LEP performances. The precision of the measurements will increase, new tests of the Standard Model will be possible and hopefully a discovery in the BSM–land. Otherwise the Large Hadron Collider will have to demonstrate that there is something beyond the celebrated Standard Model.

Acknowledgments

I am grateful to Emmanuelle Perez, Mireille Schneider, Claude Vallee, Jochen Dingfelder, Emmanuel Sauvan, Joachim Meyer for many useful discussions and fruitful collaboration. Many thanks to Joachim Meyer and Jos Vermaseren for the careful reading of the manuscript. I thank Elie Aslanides, Jean-Jacques Aubert, Phillipe Bloch, Jean-François Grivaz, Sylvain Tisserant and Jos Vermaseren for having taken part to the jury. It is a pleasure to thank also all my colleagues from the H1 collaboration. I acknowledge DESY hospitality during the completion of this work.

Bibliography

[1] E. Leader, "Spin in Particle Physics," *Cambridge Univerity Press* (2001) 234.

[2] P.Schleper private communication.

[3] **ALEPH, DELPHI,L3 and OPAL** Collaboration, "A combination of preliminary electroweak measurements and constraints on the standard model," hep-ex/0212036,SLAC-R-643, CERN-EP-2002-091, LEPEWWG-2002-02, ALEPH-2002-042-PH

[4] P. B. Renton, "Precision electroweak tests of the standard model," *Rept. Prog. Phys.* **65** (2002) 1271–1330, hep-ph/0206231.

[5] **ALEPH** Collaboration, D. Buskulic *et al.*, "Study of the four fermion final state at the Z resonance," *Z. Phys.* **C66** (1995) 3–18.

[6] **DELPHI** Collaboration, A. et al., "Measurement of the production of the four–fermion final states mediated by neutral current processes," DELPHI-NOTE-2001-096.

[7] **OPAL** Collaboration, G. Abbiendi, "Study of Z pair production and anomalous couplings in e+ e- collisions at s**(1/2) between 190-GeV and 209-GeV," hep-ex/0310013.

[8] **OPAL** Collaboration, G. Abbiendi *et al.*, "First measurement of Z/gamma* production in Compton scattering of quasi-real photons," *Phys. Lett.* **B438** (1998) 391–404, hep-ex/9808030.

[9] **DELPHI** Collaboration, P. Abreu *et al.*, "Single intermediate vector boson production in e+ e- collisions at s**(1/2) = 183-GeV and 189-GeV," *Phys. Lett.* **B515** (2001) 238–254, hep-ex/0107067.

[10] N. Arteaga-Romero, A. Jaccarini, P. Kessler, and J. Parisi, "Photon-photon collisions, a new area of experimental investigation in high-energy physics," *Phys. Rev.* **D3** (1971) 1569–1579.

[11] J. Parisi, N. Arteaga-Romero, A. Jaccarini, and P. Kessler, "Comment on the experimental investigation of photon-photon collisions in electron-positron storage rings," *Phys. Rev.* **D4** (1971) 2927–2935.

[12] **DELPHI** Collaboration, P. Abreu *et al.*, "Study of Dimuon Production in Photon-Photon Collisions and Measurement of QED Photon Structure Functions at LEP," *Eur. Phys. J.* **C19** (2001) 15–28, hep-ex/0105084.

[13] **ALEPH** Collaboration, A. et al., "Study of hadronic final states from double tagged $\gamma\gamma$ events at LEP," CERN-EP/2003-045, hep-ex/0311004.

[14] **L3** Collaboration, P. Achard *et al.*, "Double-tag events in two-photon collisions at LEP," *Phys. Lett.* **B531** (2002) 39–51, `hep-ex/0111012`.

[15] **ALEPH, L3 and OPAL** Collaboration, "Comparison of deep-inelastic electron photon scattering data with the HERWIG and PHOJET Monte Carlo models," *Eur. Phys. J.* **C23** (2002) 201–223.

[16] R. Nisius, "The photon structure from deep inelastic electron photon scattering," *Phys. Rept.* **332** (2000) 165–317, `hep-ex/9912049`.

[17] **OPAL** Collaboration, G. Abbiendi *et al.*, "Search for anomalous production of di-lepton events with missing transverse momentum in e+ e- collisions at s**(1/2) = 183-GeV - 209-GeV," `hep-ex/0309014`.

[18] **L3** Collaboration, M. Acciarri *et al.*, "Measurement of radiative Bhabha and quasi-real Compton scattering," *Phys. Lett.* **B439** (1998) 183–196.

[19] **DELPHI** Collaboration, J. et al., "Measurement of the $e^+e^- \to W^+W^-\gamma$ cross section and limits on anomalous quartic gauge couplings with DELPHI," `CERN-EP/2003-045, hep-ex/0311004`.

[20] **ALEPH** Collaboration, R. Barate *et al.*, "Search for supersymmetry in the photon(s) plus missing energy channels at s**(1/2) = 161-GeV and 172-GeV," *Phys. Lett.* **B420** (1998) 127–139, `hep-ex/9710009`.

[21] S. D. Drell and T. M. Yan *Phys.Rev.Lett.* **25** (1970) 316.

[22] **FNAL E866/NuSea** Collaboration, R. S. Towell *et al.*, "Improved measurement of the anti-d/anti-u asymmetry in the nucleon sea," *Phys. Rev.* **D64** (2001) 052002, `hep-ex/0103030`.

[23] A. D. Martin, R. G. Roberts, W. J. Stirling, and R. S. Thorne, "NNLO global parton analysis," *Phys. Lett.* **B531** (2002) 216–224, `hep-ph/0201127`.

[24] **CDF** Collaboration, F. Abe *et al.*, "Limits on quark-lepton compositeness scales from dileptons produced in 1.8-TeV p anti-p collisions," *Phys. Rev. Lett.* **79** (1997) 2198–2203.

[25] **CDF** Collaboration, T. Affolder *et al.*, "Measurement of d(sigma)/dM and forward-backward charge asymmetry for high mass Drell-Yan e+ e- pairs from p anti- p collisions at s**(1/2) = 1.8-TeV," *Phys. Rev. Lett.* **87** (2001) 131802, `hep-ex/0106047`.

[26] **CDF** Collaboration, T. Affolder *et al.*, "Search for quark lepton compositeness and a heavy W' boson using the e nu channel in p anti-p collisions at s**(1/2) = 1.8-TeV," *Phys. Rev. Lett.* **87** (2001) 231803, `hep-ex/0107008`.

[27] **CDF** Collaboration, F. Abe *et al.*, "Measurement of the lepton charge asymmetry in W boson decays produced in p anti-p collisions," *Phys. Rev. Lett.* **81** (1998) 5754–5759, `hep-ex/9809001`.

[28] E. Perez, "Searches for new phenomena at colliders," `Proceedings of ``Lepton-Photon'' Conference, Fermilab`.

[29] J. M. Campbell and R. K. Ellis, "An update on vector boson pair production at hadron colliders," *Phys. Rev.* **D60** (1999) 113006, `hep-ph/9905386`.

[30] **D0** Collaboration, B. Abbott *et al.*, "Measurement of the top quark mass in the dilepton channel," *Phys. Rev.* **D60** (1999) 052001, `hep-ex/9808029`.

[31] T. Stelzer, Z. Sullivan, and S. Willenbrock, "Single top quark production at hadron colliders," *Phys. Rev.* **D58** (1998) 094021, `hep-ph/9807340`.

[32] **CDF** Collaboration, D. Acosta *et al.*, "Search for single top quark production in p anti-p collisions at s**(1/2) = 1.8-TeV," *Phys. Rev.* **D65** (2002) 091102, `hep-ex/0110067`.

[33] **D0** Collaboration, V. M. Abazov *et al.*, "Search for single top quark production at D0 using neural networks," *Phys. Lett.* **B517** (2001) 282–294, `hep-ex/0106059`.

[34] **H1** Collaboration, C. Adloff *et al.*, "Measurement and QCD analysis of neutral and charged current cross sections at HERA," `hep-ex/0304003`.

[35] U. Baur, J. A. M. Vermaseren, and D. Zeppenfeld, "Electroweak vector boson production in high-energy ep collisions," *Nucl. Phys.* **B375** (1992) 3–44.

[36] C. Diaconu, "Parton showers effects for W production at HERA,". Prepared for Workshop on Monte Carlo Generators for HERA Physics (Plenary Starting Meeting), Hamburg, Germany, 27-30 Apr 1998.

[37] K.-P. O. Diener, C. Schwanenberger, and M. Spira, "Photoproduction of W bosons at HERA: QCD corrections," *Eur. Phys. J.* **C25** (2002) 405–411, `hep-ph/0203269`.

[38] K.-P. O. Diener, C. Schwanenberger, and M. Spira, "Photoproduction of W bosons at HERA: Reweighting method for implementing QCD corrections in Monte Carlo programs," `hep-ex/0302040`.

[39] M. Spira, "W boson production at NLO," `hep-ph/9905469`.

[40] P. Nason, R. Ruckl, and M. Spira, "A note on W boson production at HERA," *J. Phys.* **G25** (1999) 1434–1435, `hep-ph/9902296`.

[41] **H1** Collaboration, T. Ahmed *et al.*, "Observation of an e+ p $\to$ mu+ X event with high transverse momenta at HERA,". DESY-94-248.

[42] **H1** Collaboration, C. Adloff *et al.*, "Observation of events with an isolated high energy lepton and missing transverse momentum at HERA," *Eur. Phys. J.* **C5** (1998) 575–584, `hep-ex/9806009`.

[43] **H1** Collaboration, V. Andreev *et al.*, "Isolated electrons and muons in events with missing transverse momentum at HERA," *Phys. Lett.* **B561** (2003) 241–257, `hep-ex/0301030`.

[44] M. Schneider, "Recherche d'evenements contenant un lepton isole et de l'impulsion trans- verse manquante sur le collisionneur HERA avec le detecteur H1," *PhD thesis, University of Strasbourg, DESY-THESIS-2003-013* (2003).

[45] **ZEUS** Collaboration, S. Chekanov *et al.*, "Search for single-top production in ep collisions at HERA," *Phys. Lett.* **B559** (2003) 153–170, `hep-ex/0302010`.

[46] **ZEUS** Collaboration, "Isolated tau leptons in events with large missing transverse momentum at HERA," `hep-ex/0311028`.

[47] J. Dingfelder, “Anomalous top production in ep collisions at HERA,” *PhD thesis, University of Heidelberg* (2002).

[48] D. Dannheim, “Search for events with isolated leptons and large missing transverse momentum in ep collision at HERA,” *PhD thesis, University of Hamburg, DESY-THESIS-2003-025* (2003).

[49] T. Carli, D. Dannheim, and L. Bellagamba, “Observation of events with isolated leptons and large missing transverse momentum at HERA,” *in preparation* (2004).

[50] C. Bacci *et al. Lett. Nouvo Cimento* **3** (1972) 703.

[51] G. Barbiellini *et al.*, “MUON PAIR PRODUCTION BY PHOTON - PHOTON INTERACTION IN THE ADONE e+ e- STORAGE RING,” *Phys. Rev. Lett.* **32** (1974) 385.

[52] R. L. Jaffe, “PHOTOPRODUCTION OF MASSIVE MUON PAIRS AT HIGH-ENERGIES,” *Phys. Rev.* **D4** (1971) 1507.

[53] A. C. Bawa, K. Charchula, and W. J. Stirling, “Photoproduction of large mass lepton pairs at HERA as a probe of the small x structure of the proton,” *Phys. Lett.* **B313** (1993) 461–468, `hep-ph/9307340`.

[54] N. Arteaga-Romero, C. Carimalo, and P. Kessler, “High P(t) lepton pair production at e p colliders: Comparison between various production mechanisms,” *Z. Phys.* **C52** (1991) 289–296.

[55] D. Hoffmann and L. Favart, “Lepton pair Monte Carlo generators for HERA physics,”. Contributed to the Proceedings of the Workshop on Monte Carlo Generators for HERA Physics (Plenary Starting Meeting), Hamburg, Germany, 27-30 Apr 1998.

[56] J. A. M. Vermaseren, “TWO PHOTON PROCESSES AT VERY HIGH-ENERGIES,” *Nucl. Phys.* **B229** (1983) 347.

[57] S. P. Baranov, O. Duenger, H. Shooshtari, and J. A. M. Vermaseren, “LPAIR: A generator for lepton pair production,”. In *Hamburg 1991, Proceedings, Physics at HERA, vol. 3* 1478-1482. (see HIGH ENERGY PHYSICS INDEX 30 (1992) No. 12988).

[58] T. Abe, “GRAPE-Dilepton (Version 1.1): A generator for dilepton production in e p collisions,” *Comput. Phys. Commun.* **136** (2001) 126–147, `hep-ph/0012029`.

[59] **H1** Collaboration, A. Aktas *et al.*, “Multi-electron production at high transverse momenta in e p collisions at HERA,” *Eur. Phys. J.* **C31** (2003) 17–29, `hep-ex/0307015`.

[60] **H1** Collaboration, A. Aktas *et al.*, “Muon Pair Production in ep Collisions at HERA,” `hep-ex/0311015`.

[61] **ZEUS** Collaboration, “Study of multi-lepton production with the ZEUS detector at HERA,” *Contributed paper* **910** *to XXXIst ICHEP, Amsterdam* (2003).

[62] M. Kuze and Y. Sirois, “Search for particles and forces beyond the standard model at HERA e p and Tevatron p anti-p colliders,” *Prog. Part. Nucl. Phys.* **50** (2003) 1–62, `hep-ex/0211048`.

[63] G. Senjanovic and R. N. Mohapatra, “EXACT LEFT-RIGHT SYMMETRY AND SPONTANEOUS VIOLATION OF PARITY,” *Phys. Rev.* **D12** (1975) 1502.

[64] R. N. Mohapatra and R. E. Marshak, “LOCAL B-L SYMMETRY OF ELECTROWEAK INTERACTIONS, MAJORANA NEUTRINOS AND NEUTRON OSCILLATIONS,” *Phys. Rev. Lett.* **44** (1980) 1316–1319.

[65] R. N. Mohapatra and G. Senjanovic, “Neutrino mass and spontaneous parity nonconservation,” *Phys. Rev. Lett.* **44** (1980) 912.

[66] **OPAL** Collaboration, G. Abbiendi *et al.*, “Search for doubly charged Higgs bosons with the OPAL detector at LEP,” *Phys. Lett.* **B526** (2002) 221–232, `hep-ex/0111059`.

[67] **H1** Collaboration, “Search for doubly charged Higgs production at HERA,” `Contributed paper` **104** `to EPS03, Aachen, http://www-h1.desy.de/h1/www/publication`

[68] **OPAL** Collaboration, G. Abbiendi *et al.*, “Search for the single production of doubly-charged Higgs bosons and constraints on their couplings from Bhabha scattering,” `hep-ex/0308052`.

[69] F. Cuypers and S. Davidson, “Bileptons: Present limits and future prospects,” *Eur. Phys. J.* **C2** (1998) 503–528, `hep-ph/9609487`.

[70] **ALEPH** Collaboration, A. Heister *et al.*, “Search for charged Higgs bosons in e+ e- collisions at energies up to s**(1/2) = 209-GeV,” *Phys. Lett.* **B543** (2002) 1–13, `hep-ex/0207054`.

[71] K. Hagiwara, D. Zeppenfeld, and S. Komamiya, “EXCITED LEPTON PRODUCTION AT LEP AND HERA,” *Z. Phys.* **C29** (1985) 115.

[72] **H1** Collaboration, C. Adloff *et al.*, “Search for excited neutrinos at HERA,” *Phys. Lett.* **B525** (2002) 9–16, `hep-ex/0110037`.

[73] **H1** Collaboration, C. Adloff *et al.*, “Search for excited electrons at HERA,” *Phys. Lett.* **B548** (2002) 35–44, `hep-ex/0207038`.

[74] H. Spiesberger, M. Spira, and P. M. Zerwas, “The standard model: Physical basis and scattering experiments,” `hep-ph/0011255`.

[75] R. M. Godbole, “Physics potential of the next generation colliders,” `hep-ph/0205114`.

[76] K. Hagiwara, R. D. Peccei, D. Zeppenfeld, and K. Hikasa, “PROBING THE WEAK BOSON SECTOR IN e+ e- $\to$ W+ W-,” *Nucl. Phys.* **B282** (1987) 253.

[77] **ALEPH** Collaboration, A. Heister *et al.*, “Measurement of triple gauge boson couplings at LEP energies up to 189-GeV,” *Eur. Phys. J.* **C21** (2001) 423–441, `hep-ex/0104034`.

[78] **ALEPH** Collaboration, T. Barklow, S. Jezequel, and J. B. Hansen, “Measurement of triple gauge boson couplings in e+ e- collisions up to 208-GeV,”. SLAC-REPRINT-2001-047.

[79] **D0** Collaboration, S. Abachi *et al.*, “Limits on anomalous W W gamma couplings from p anti-p –¿ W gamma + X events at s**(1/2) = 1.8-GeV,” *Phys. Rev. Lett.* **78** (1997) 3634–3639, `hep-ex/9612002`.

[80] **ZEUS** Collaboration, J. Breitweg *et al.*, “W production and the search for events with an isolated high-energy lepton and missing transverse momentum at HERA,” *Phys. Lett.* **B471** (2000) 411–428, `hep-ex/9907023`.

[81] U. Baur and D. Zeppenfeld, “MEASURING THE W W gamma VERTEX IN SINGLE W PRODUCTION AT e p COLLIDERS,” *Nucl. Phys.* **B325** (1989) 253.

[82] T. Stelzer, Z. Sullivan, and S. Willenbrock, “Single-top-quark production via W-gluon fusion at next-to- leading order,” *Phys. Rev.* **D56** (1997) 5919–5927, `hep-ph/9705398`.

[83] S. Moretti and K. Odagiri, “Single-top production at future e p colliders,” *Phys. Rev.* **D57** (1998) 3040–3050, `hep-ph/9709435`.

[84] K. Hagiwara, M. Tanaka, and T. Stelzer, “Single top production at LEP-200,” *Phys. Lett.* **B325** (1994) 521–525, `hep-ph/9401295`.

[85] T. Han and J. L. Hewett, “Top charm associated production in high energy e+ e- collisions,” *Phys. Rev.* **D60** (1999) 074015, `hep-ph/9811237`.

[86] **H1** Collaboration, A. Aktas *et al.*, “Search for single top quark production in ep collisions at HERA,” `hep-ex/0310032`.

[87] **CDF** Collaboration, F. Abe *et al.*, “Search for flavor-changing neutral current decays of the top quark in p anti-p collisions at s**(1/2) = 1.8-TeV,” *Phys. Rev. Lett.* **80** (1998) 2525–2530.

[88] T. Han, R. D. Peccei, and X. Zhang, “Top quark decay via flavor changing neutral currents at hadron colliders,” *Nucl. Phys.* **B454** (1995) 527–540, `hep-ph/9506461`.

[89] **L3** Collaboration, P. Achard *et al.*, “Search for single top production at LEP. ((B)),” *Phys. Lett.* **B549** (2002) 290–300, `hep-ex/0210041`.

[90] **ALEPH** Collaboration, A. Heister *et al.*, “Search for single top production in e+ e- collisions at s**(1/2) up to 209-GeV,” *Phys. Lett.* **B543** (2002) 173–182, `hep-ex/0206070`.

[91] **OPAL** Collaboration, G. Abbiendi *et al.*, “Search for single top quark production at LEP2,” *Phys. Lett.* **B521** (2001) 181–194, `hep-ex/0110009`.

[92] **H1** Collaboration, C. Adloff *et al.*, “Searches at HERA for squarks in R-parity violating supersymmetry,” *Eur. Phys. J.* **C20** (2001) 639–657, `hep-ex/0102050`.

[93] **H1** Collaboration, “Searches for Squark Production in R-Parity Violating Supersymmetry at HERA,”.

[94] J. Kalinowski, R. Ruckl, H. Spiesberger, and P. Zerwas, “Speculations on SUSY Mechanisms of Isolated μ^+ Production in ep Collisions,” `unpublished`.

[95] C. Diaconu, J. Kalinowski, T. Matsushita, H. Spiesberger, and D. S. Waters, “High p(T) leptons and W production at HERA,” *J. Phys.* **G25** (1999) 1412–1417, `hep-ph/9901335`.

[96] T. Kon, J.-i. Kamoshita, T. Kobayashi, S. Kitamura, and Y. Kurihara, “Scalar neutrino production in R-parity violating supersymmetric model at HERA,” `hep-ph/0203262`.

[97] **D0** Collaboration, B. Abbott *et al.*, “A quasi-model-independent search for new physics at large transverse momentum,” *Phys. Rev.* **D64** (2001) 012004, `hep-ex/0011067`.

[98] **H1** Collaboration, “General Search for New Phenomena at HERA,” *Contributed paper* **108** *to EPS03, Aachen, http://www-h1.desy.de/h1/www/publications/htmlsplit/H1prelim-03-063.long.html* (2003).